第18回 若手科学者によるプラズマ研究会　主題：プラズマ計測・制御技術の結集
＠平成２７年３月４～６日 日本原子力研究開発機構 那珂核融合研究所

マイクロ波-ミリ波-テラヘルツ波を用いた磁場閉じ込め核融合プラズマ計測

徳沢季彦

核融合科学研究所

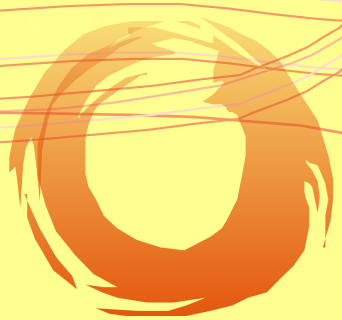

資料協力：長山、久保、田中、秋山（核融合研）、西浦（東大）

Contents

- はじめに
- 干渉計
  - マイクロ波干渉計、FIRレーザー干渉計、分散干渉計
- 反射計
  - ドップラー反射計、パルスレーダー
- 協同トムソン散乱
- まとめ

ITER Diagnostics

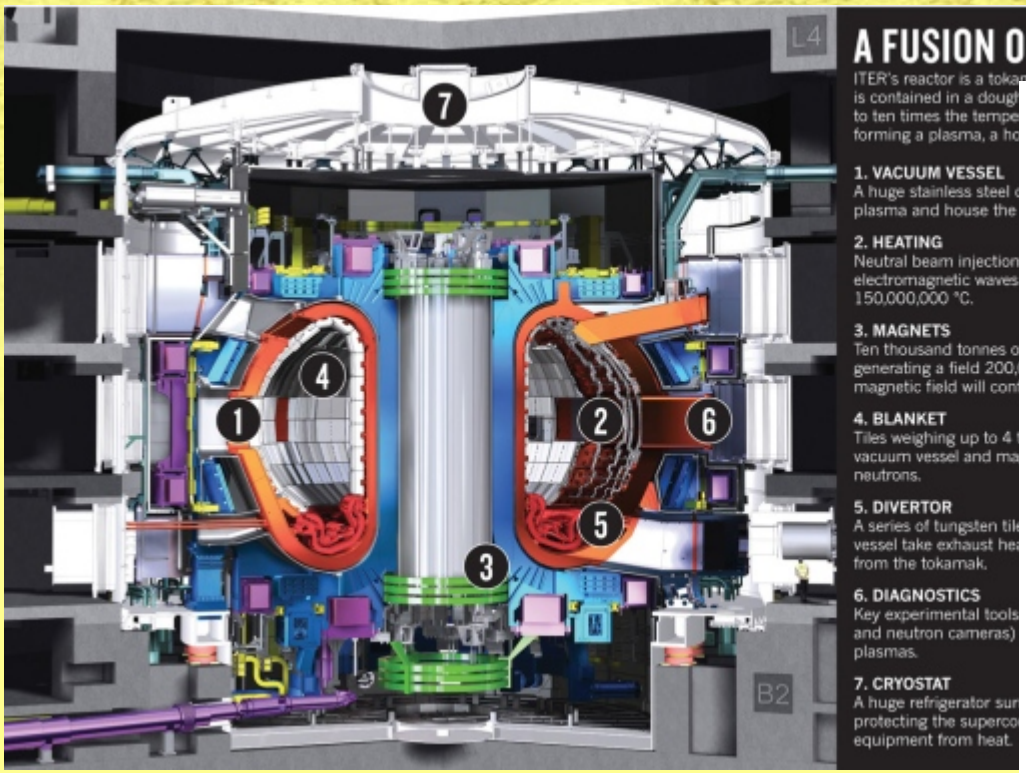

The diagnostics system will comprise about 50 individual measuring systems drawn from the full range of modern plasma diagnostic techniques, including lasers, X-rays, neutron cameras, impurity monitors, particle spectrometres, radiation bolometers, pressure and gas analysis, and optical fibres.

Magnetic Diagnostics	Spectroscopic and NPA Systems
Vessel Magnetics	CXRS Active Spectroscopy (+DNB)
In-vessel magnetics	H Alpha Spectroscopy
Divertor Coils	VUV Impurity Monitoring (Main Plasma)
Continuous Rogowski Coils	Visible & UV Impurity Monitoring (Divertor)
Diamagnetic Loop	X-Ray Crystal Spectrometers
Halo Current Sensors	Visible Continuum Array
Neutron Diagnostics	Soft X-Ray Array
Radial Neutron Camera	Neutral Particle Analyzers
Vertical Neutron Camera	Laser Induced Fluorescence
Microfission chambers (in-vessel)	MSE based on Heating Beam
Neutron Flux Monitors (ex-vessel)	**Microwave Diagnostics**
Gamma-Ray Spectrometers	ECE Diagnostics for Main Plasma
Neutron Activation Systems	Reflectometers for Main Plasma
Lost Alpha Detectors	Reflectometers for Plasma Position
Knock-on Tail Neutron Spectrometer	Reflectometers for Divertor Plasma
Optical/IR Systems	ECA for Divertor Plasma
Thomson Scattering (Core)	Microwave Scattering (Main Plasma)
Thomson Scattering (Edge)	Fast Wave Reflectometry
Thomson Scattering (X-point)	**Plasma-Facing Component & Operational Diagnostics**
Thomson Scattering (Divertor)	IR Cameras, visible/IR TV
Toroidal interferometer/Polarimeter	Thermocouples
Poloidal Polarimeter	Pressure Gauges
Collective Thomson scattering	Residual Gas Analyzers
Bolometric Systems	IR Thermography Divertor
Bolometric Array (Main Plasma)	Langmuir Probes
Bolometric Array (Divertor)	

Table 1. Overview of the diagnostics foreseen at ITER

A.J.H. Donne, FST, 61, 357 (2012)

将来の核燃焼炉でも電磁波計測は有用

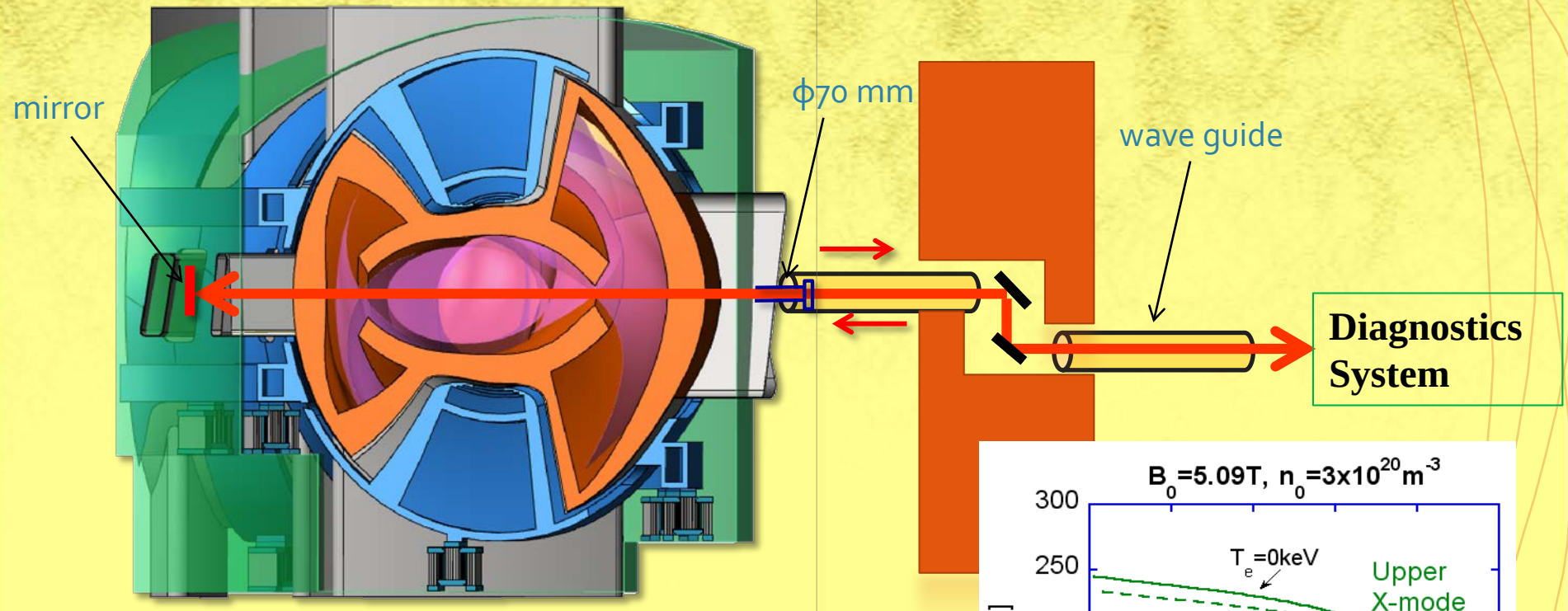

- ✓ 迷路構造の伝送導波路の適用可
- ✓ 狭小な真空窓でのアクセスに対応可
- ✓ 高信頼性の確立

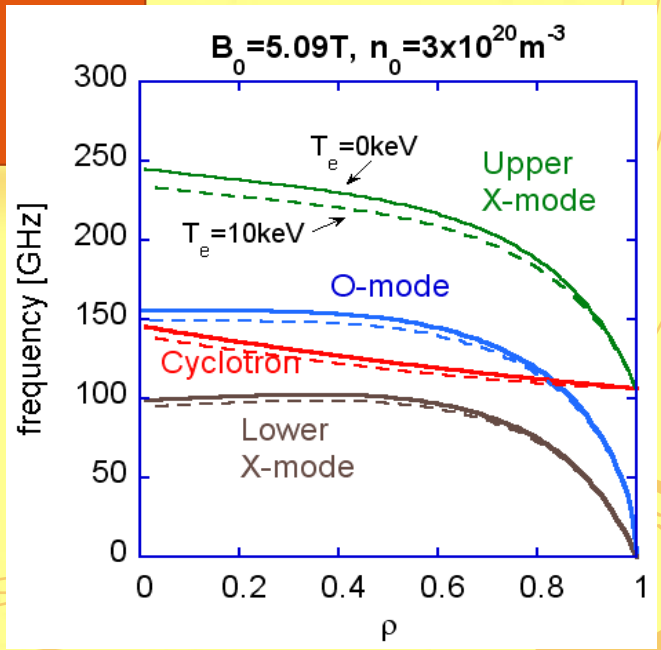

計測器への要求

- 高精度化：精緻な計測システムにより、新しい物理の解明に貢献
- 高信頼化：安定な運転制御のために必要なパラメータの提供

Real-time diagnostic / system integration

AUGの計測例

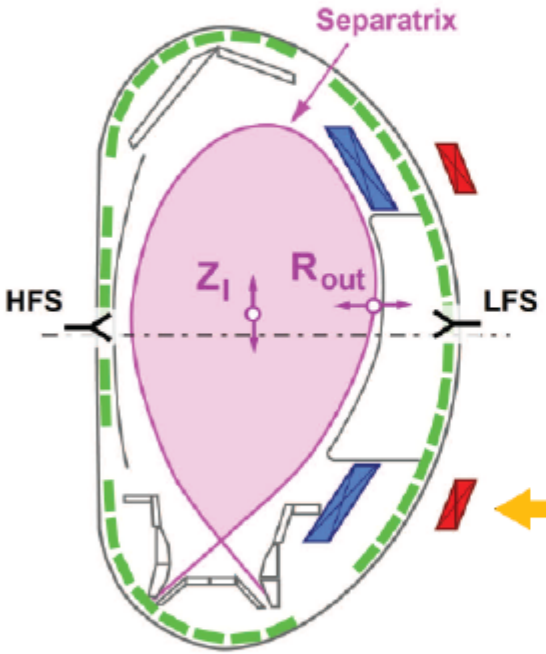

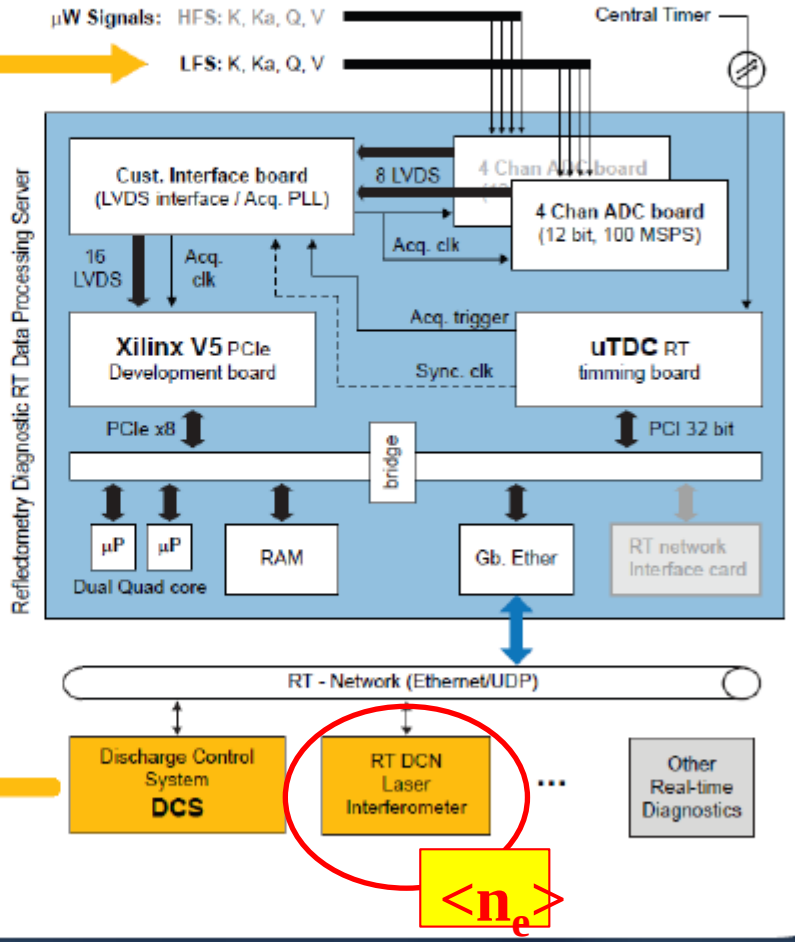

Reflectometry PP demonstration on AUG

J.Santos

L-mode 、H-mode（type-I ELM付）における位置制御に成功

First demonstration discharge

Reflectometry control during separate L and H-mode phases

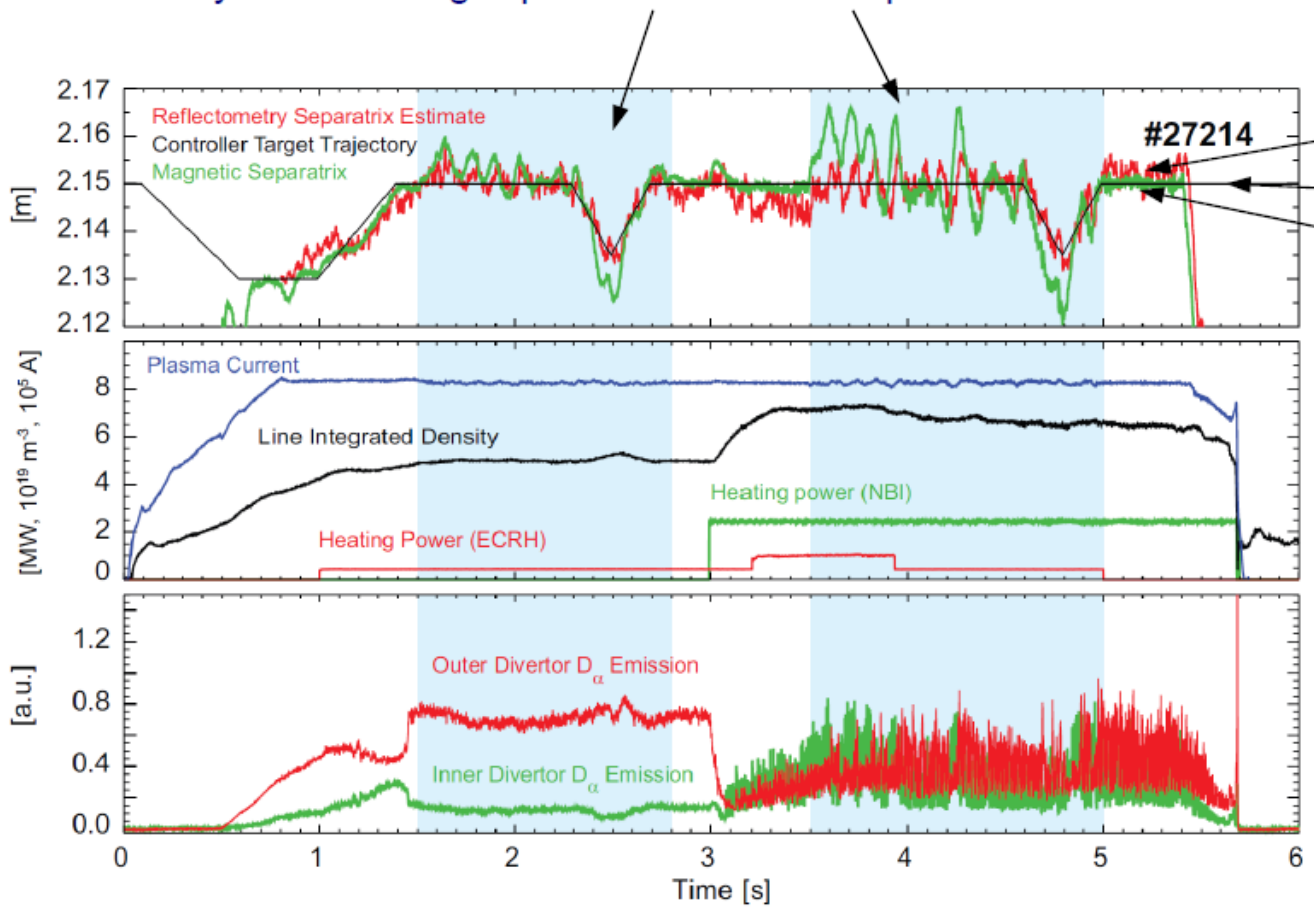

- R_{out}: outer (LFS) plasma position

Reflectometer

Requested

Magnetic

- Refl. tracks mag. during non-control phases (ramp-up & down)
- Refl. maintains good control when in change – even during programed radial movement
- Overshots in mag. signal t.b. resolved

Contents

- はじめに
- 干渉計
  - マイクロ波干渉計、FIRレーザー干渉計、分散干渉計
- 反射計
  - ドップラー反射計、パルスレーダー
- 協同トムソン散乱
- まとめ

Principle of interferometer for electron density measurements

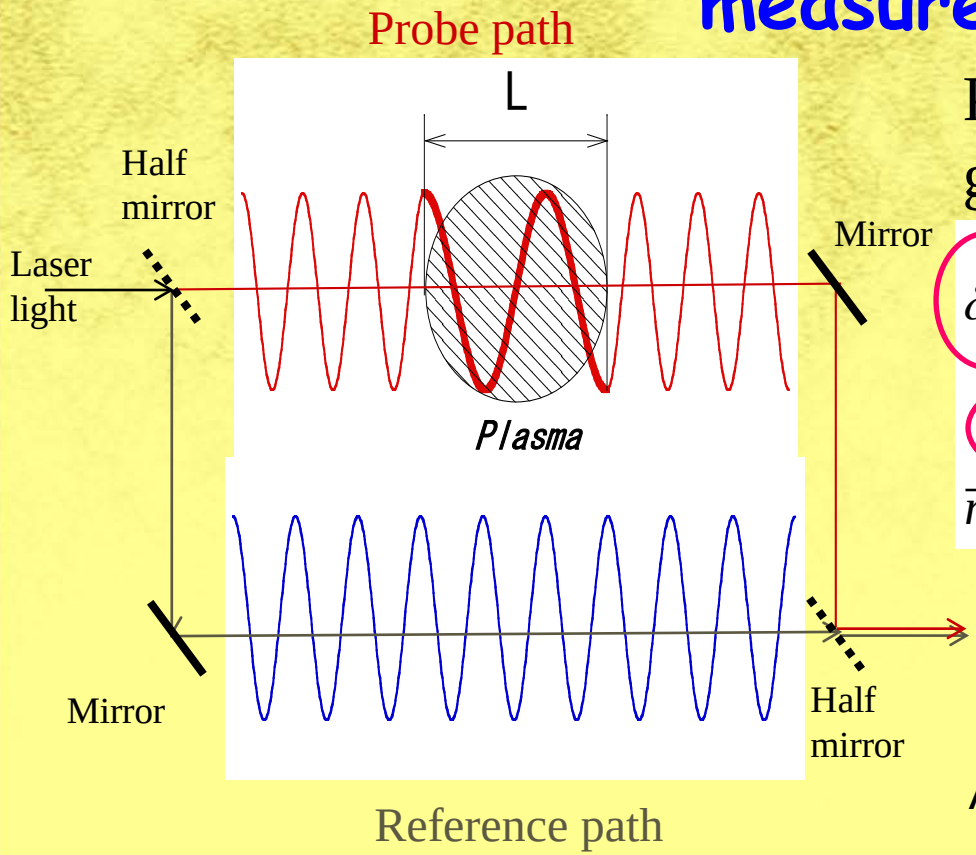

Phase difference with plasma is given by

$$\delta\phi = \mathrm{k}\delta\mu\, L = 2\pi\frac{\delta\mu\, L}{\lambda} = \frac{2\pi}{\lambda}\frac{1}{2}\frac{\lambda^2 e^2}{4\pi c^2 \varepsilon_0 m_e}\bar{n}L$$

$$\propto \lambda\, \bar{n}\, L$$

$\bar{n}$; line averaged electron density

Since, $\delta\phi \propto \lambda, \delta\phi \propto \omega^{-1}$

As long as $\omega >> \omega_p, \omega_c$ is satisfied.

longer wavelength (lower frequency) is preferable to get larger phase shift.

Effective path difference due to the existence of plasma gives electron density of plasma.

低密度プラズマ → マイクロ波、ミリ波
高密度プラズマ → FIR、IR

Interferometer for 1/3 scaled Negative Ions Source

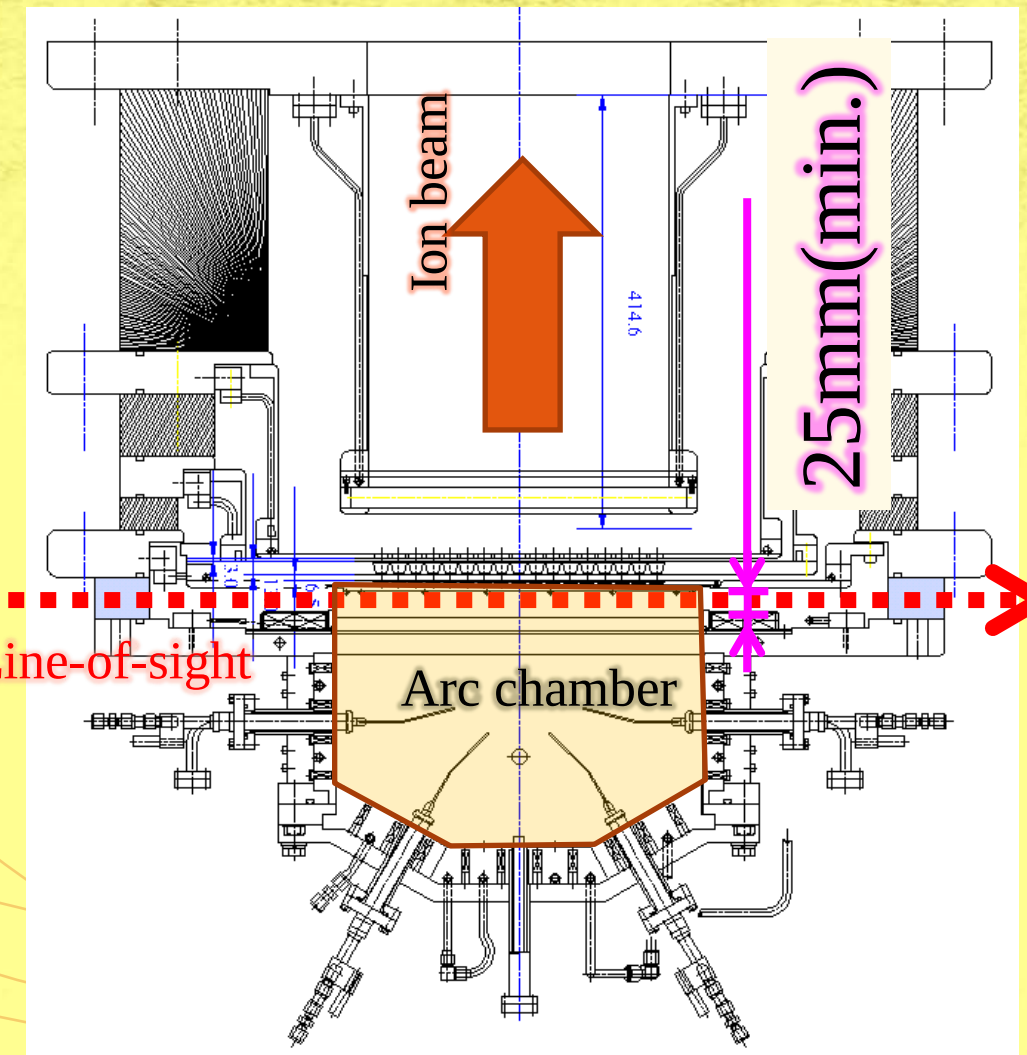

[目的]
NBI負イオン源内における、Cs添加➔負イオン増大時の電子密度の減少量の計測

ターゲット電子密度：$10^{16\sim17}m^{-3}$

[課題]
- ✓ 狭小なアクセス路➔金属導波管
- ✓ 加速高電圧印加➔ 絶縁導波
- ✓ 干渉計波長の選択➔ミリ波
- ✓ 位相計測➔高感度1/2000フリンジ位相計

Millimeter wave interferometer

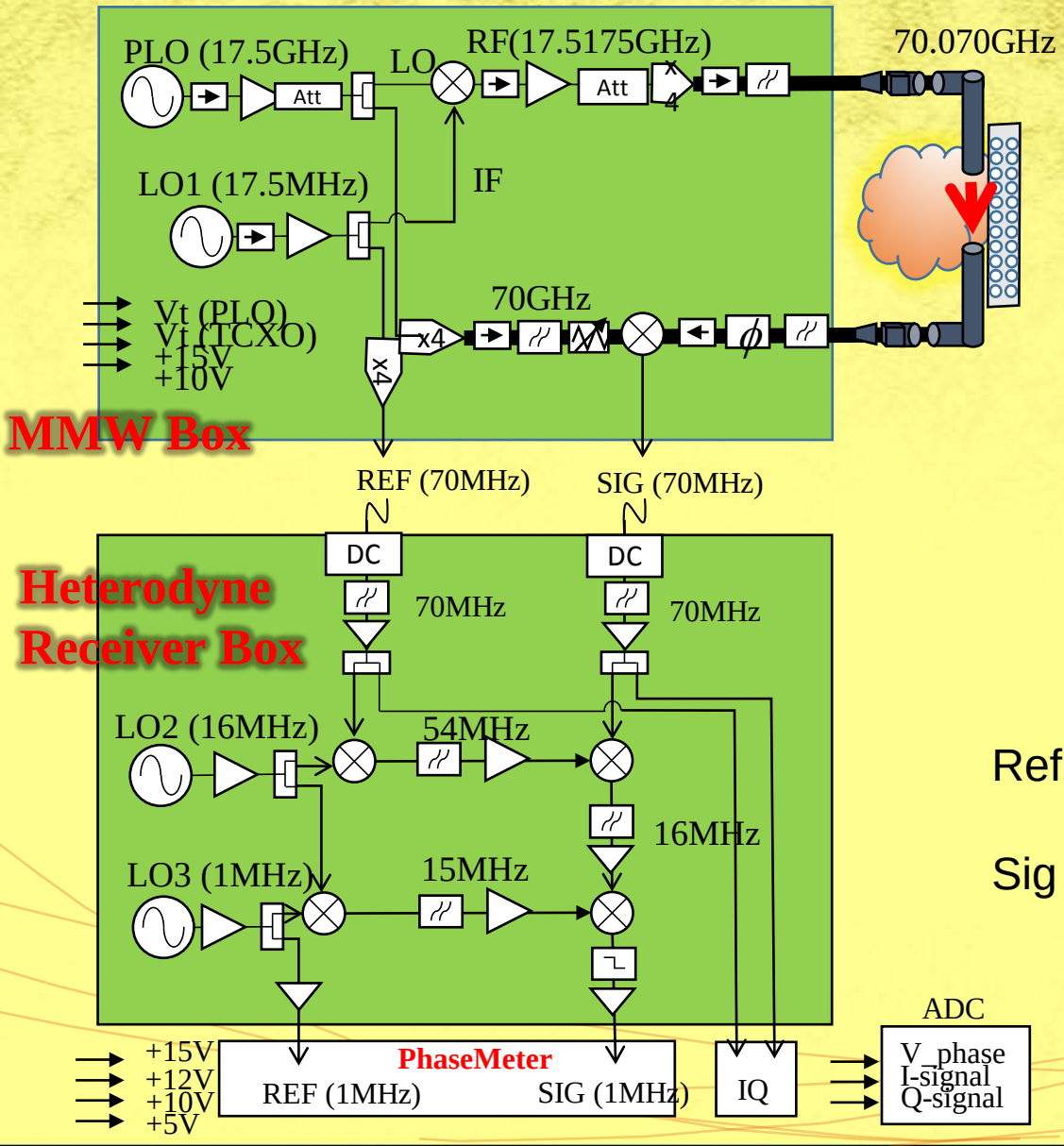

SSBM

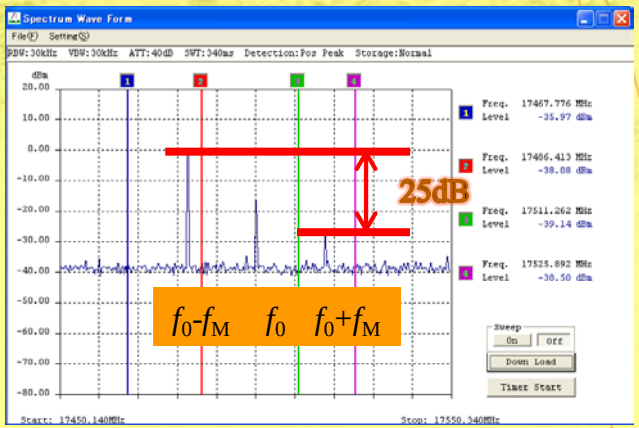

Heterodyne receiver output

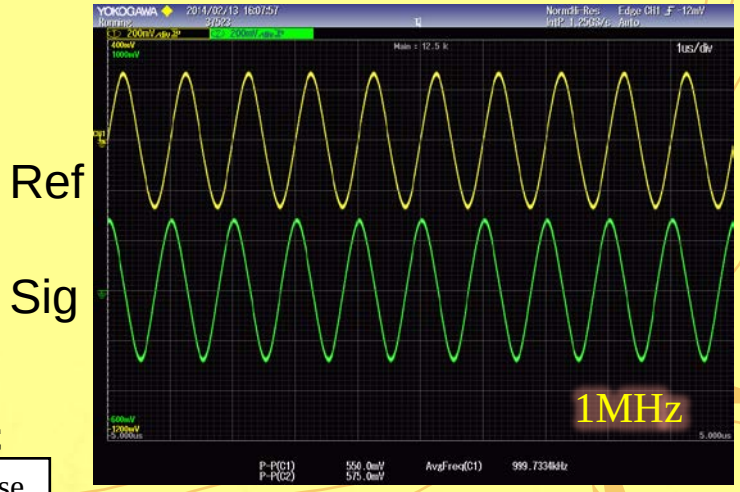

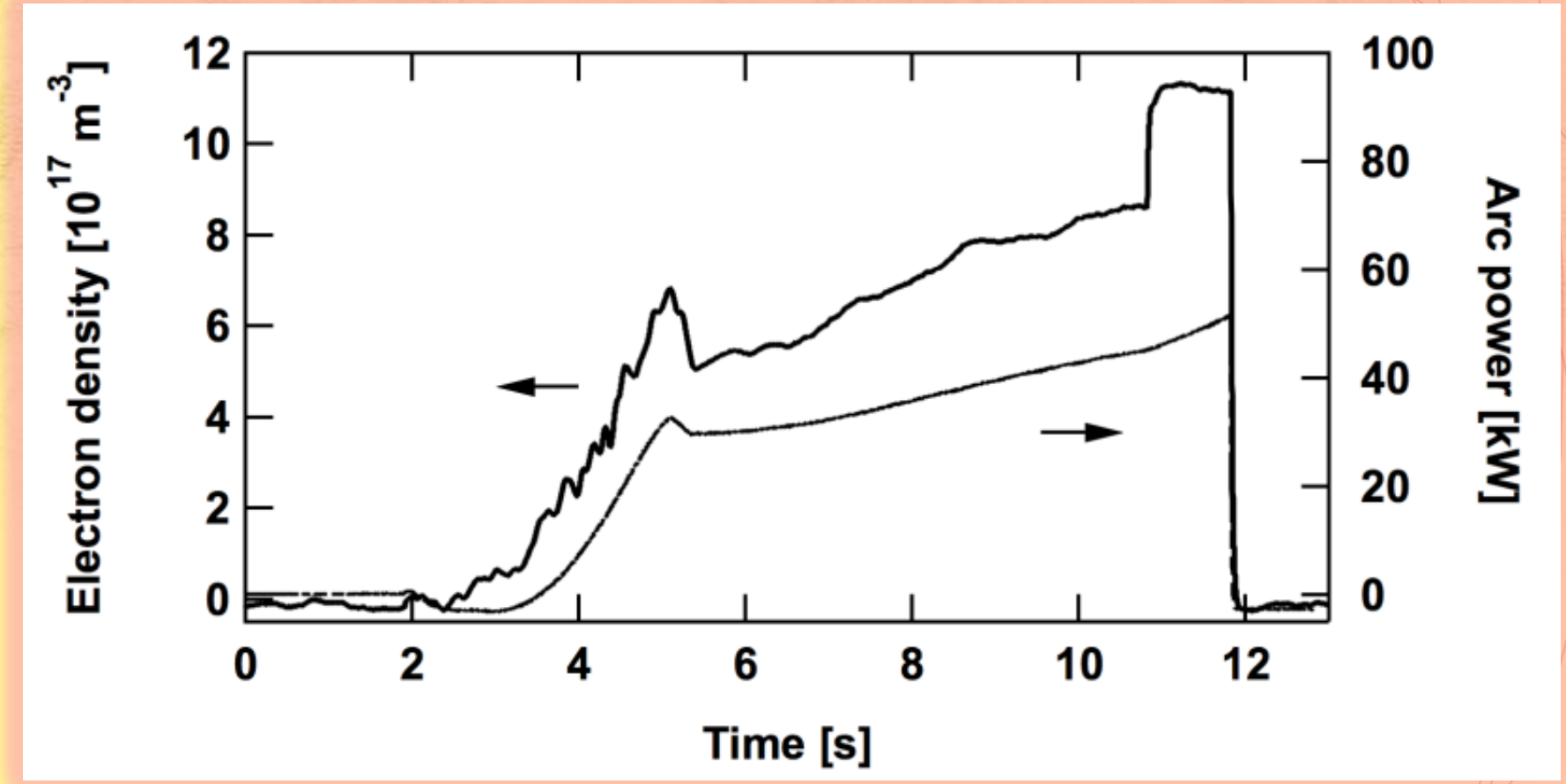

Figure 1 shows the time evolution of the electron density obtained with improved millimeter-wave interferometer in the pure hydrogen plasma. The beam was extracted from 10.8 s to 11.8 s. The electron density changes with the arc power and rapidly rises when the extraction voltage is applied. Amount of the electron density change before and after the beam extraction is 2.6 ×10^{17} m^{-3}. It has been observed that the negative ion density shows the different response to the extraction voltage and it rapidly drops with beam extraction.

Choice of probe beam wavelength

- Low frequency (long wavelength) limit
  - Refraction problem due to plasma density gradient sets the long wavelength limit

$$d = 2\left(\frac{\lambda Z_o}{\pi}\right)^{1/2} \rightarrow Z_o \alpha_m \leq 2\left(\frac{\lambda Z_o}{\pi}\right)^{1/2}$$

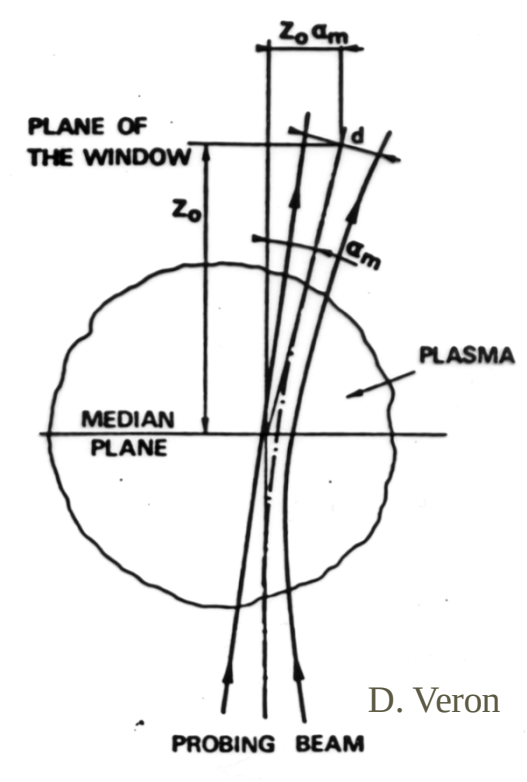

$$\alpha_m = \sin^{-1}\left(\frac{n_o}{n_c}\right) \cong \frac{n_o}{n_c} = 8.97 \times 10^{-16} n_o \lambda^2$$

$$\lambda \leq 1.16 \times 10^{10} (Z_o n_o^2)^{-1/3} m$$

- *Example: Z_o = 3.8 m, $n_e(0)$ = 2x10^{20}/m^3 leads to λ< 210 μm*

波長が長いほど、屈折の効果が大きい。

119-μm CH_3OH Laser System on LHD

CO2 laser pumped CH3OH twin laser is used.
Wavelength is 118.8μm.

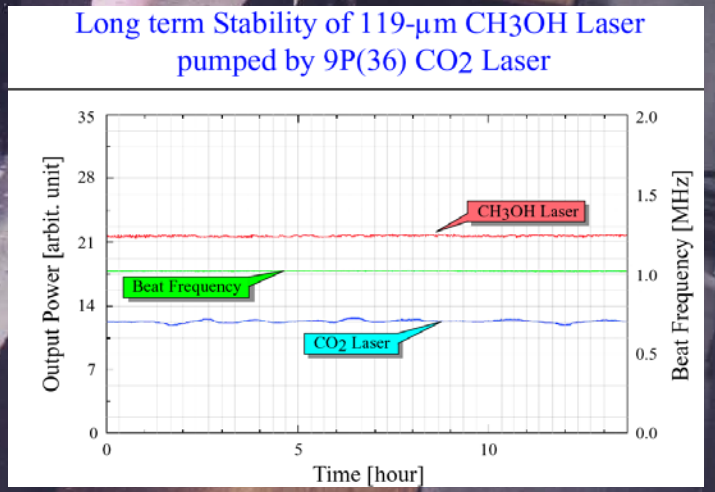

Cross Sectional View of the LHD Exp. Room

$$\Delta\phi = 2.8 \times 10^{-15}\lambda \int_{Y_1}^{Y_2} n_e(r)\,dy + \frac{3.9 \times 10^{-29}}{\lambda} \int_{Y_1}^{Y_2} n_n(r)\,dy + \frac{2\pi\Delta L}{\lambda}$$

振動成分

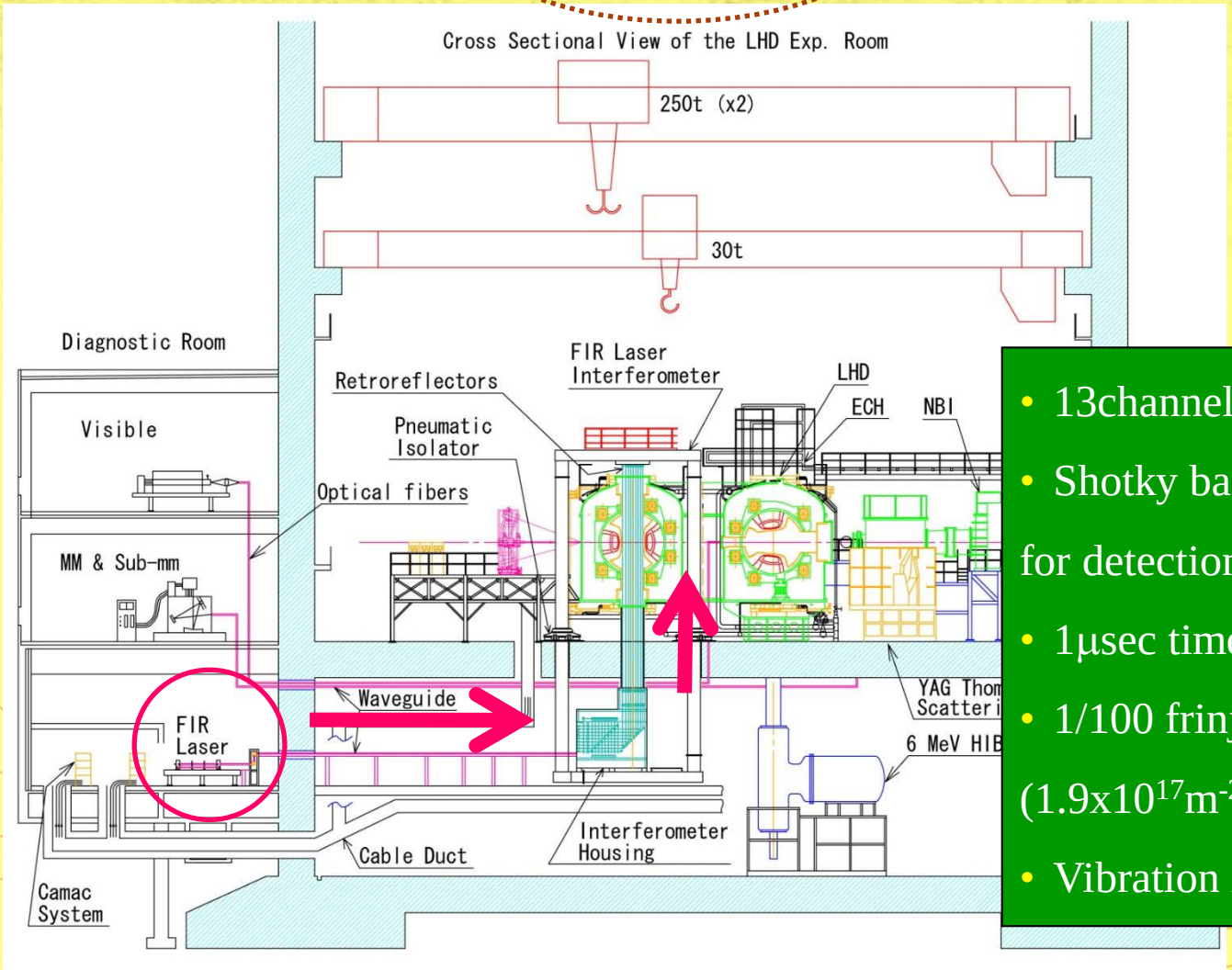

- 13channels 90mm spacing.
- Shotky barrier diodes are used for detection
- 1μsec time resolution.
- 1/100 frinje resolution ($1.9 \times 10^{17} m^{-2}$)
- Vibration is negligible.

電子密度の再構成分布の例

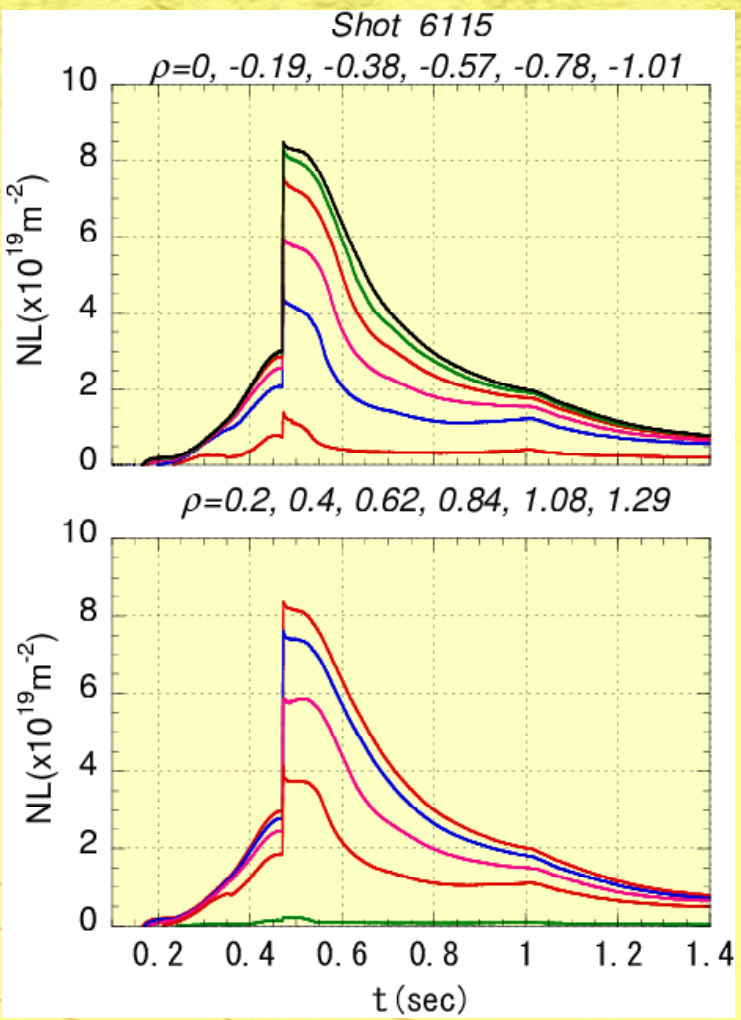

Density profile

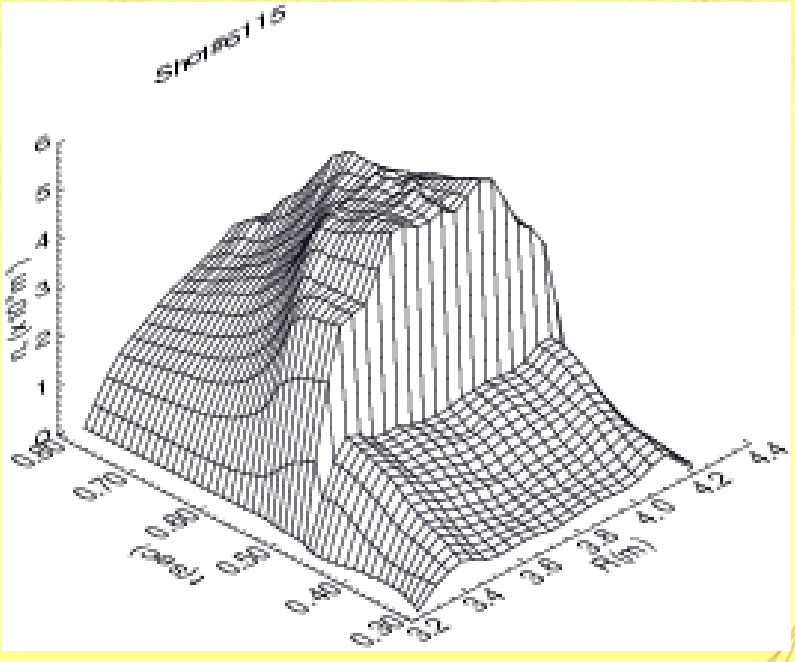

Change of Density profiles after single pellete injection.Rax=3.75m, Bt=1.5T ,NBI heated

1. What is dispersion interferometer?

Conventional Interferometer

(for electron density measurement)

Advantages

1. High temporal and density resolutions
2. Widely used (well matured technique)

Disadvantages

1. Errors due to mechanical vibrations

solution

- Vibration isolation system
- Two color interferometer

2. Fringe jump errors in high density range

solution

Short-wavelength lasers (57 μm, 10 μm)

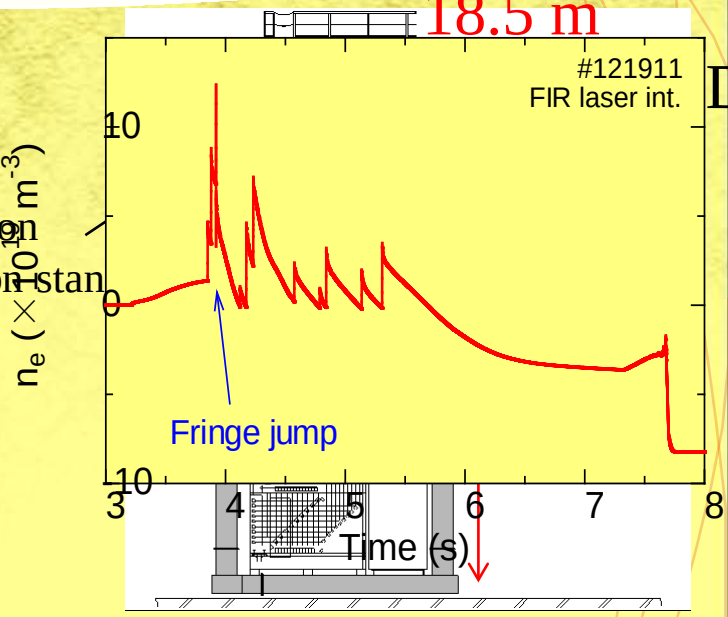

***One of the fundamental solutions is a* Dispersion Interferometer (DI)**

V. P. Drachev *et. al.*, RSI **64** 1010 (1993)., P. A. Bagryansky *et. al.*, RSI **77** 053501 (2006).

low sensitivity to vibrations, no fringe jumps (by selecting appropriate wavelength)

DI is attractive for high density, large and steady-state fusion devices

2. Principle of Basic Dispersion Interferometer (DI)

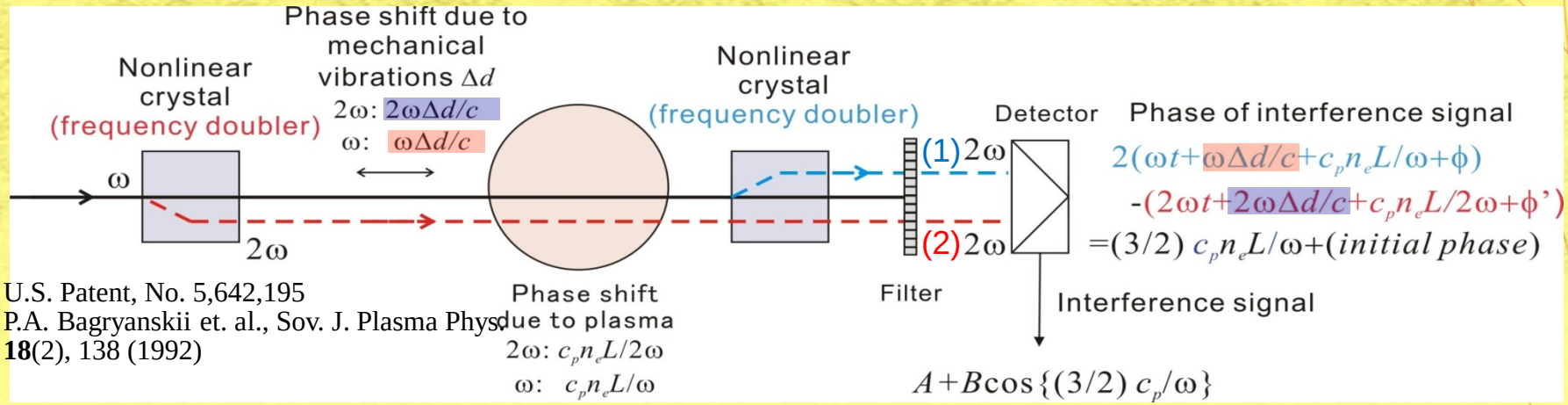

U.S. Patent, No. 5,642,195
P.A. Bagryanskii et. al., Sov. J. Plasma Phys. **18**(2), 138 (1992)

Phases of 2nd harmonic beams

$$(1):\ 2(\omega t+\omega\Delta d/c+c_p\bar{n}_e L/\omega+\phi_1)\equiv\varphi_1$$
$$(2):\ 2\omega t+2\omega\Delta d/c+c_p\bar{n}_e L/(2\omega)+\phi_2\equiv\varphi_2$$

(c_p: Constant)

Interference signal between two 2nd harmonics

$$I=A+B\cos(\varphi_1-\varphi_2)=A+B\cos\left(\frac{3}{2}\frac{c_p\bar{n}_e L}{\omega}+\phi\right)$$

$A=I_1+I_2,\ B=2\sqrt{I_1 I_2}$

I_1, I_2 : intensities of 2nd harmonics

ϕ : initial phase

Phases due to mechanical vibrations are cancelled automatically and only those due to plasma dispersion remain in the interference signal.

3. CO_2 laser (10 μm) DI on LHD

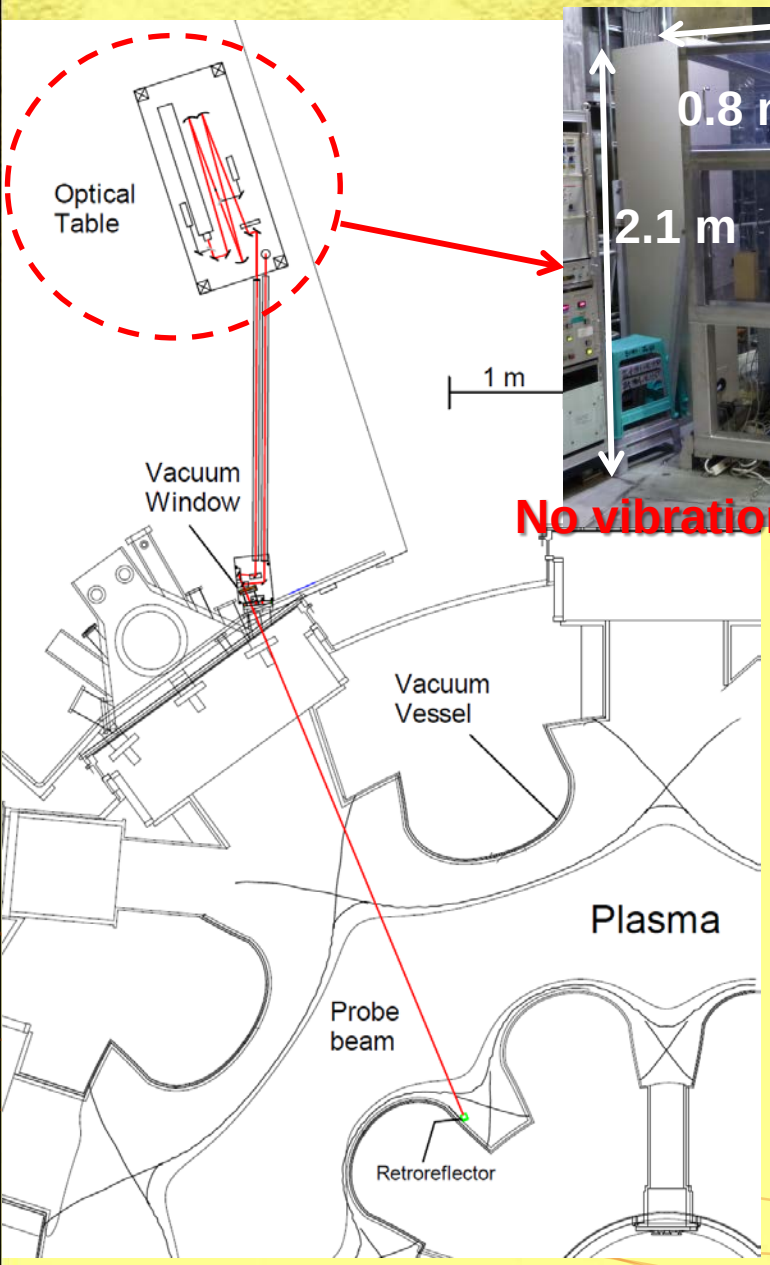

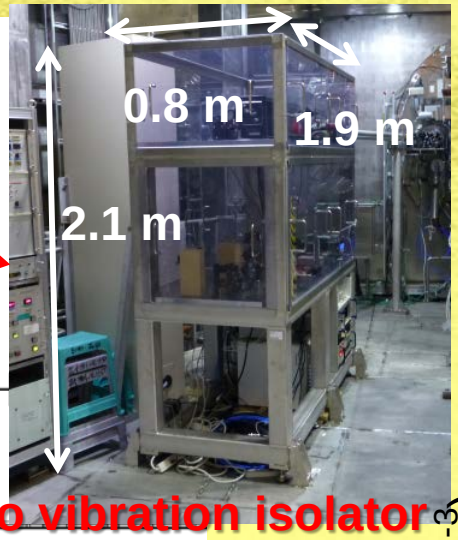

No vibration isolator

- **Line density resolution on LHD:**
  8×10^{17} m^{-2} (2.5×10^{17} m^{-3}) for 3000 s
  4×10^{17} m^{-2} (1.3×10^{17} m^{-3}) for 100 s
- **Temporal resolution:100 μs**
- **Latency: 100 μs**

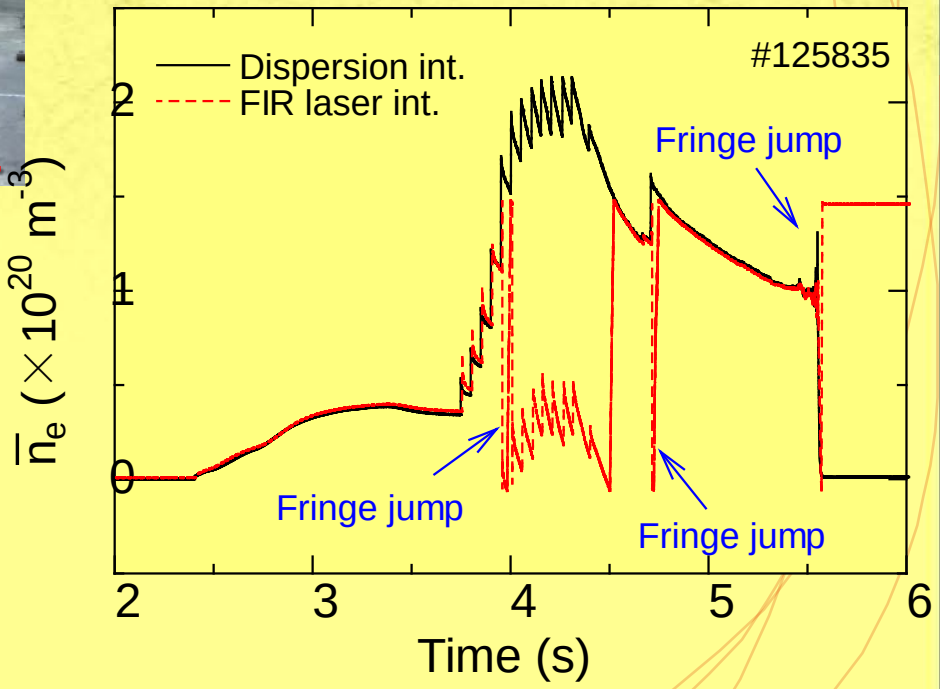

Fringe shift @ 10.6 μm> 1 fringe: risk of fringe jump

However, number of fringe shift is small (~ 3 fringes), fast sampling (100 kHz on LHD) can track the fringe shift and can avoid the fringe jumps.

Contents

- はじめに
- 干渉計
  - マイクロ波干渉計、FIRレーザー干渉計、分散干渉計
- 反射計
  - ドップラー反射計、パルスレーダー
- 協同トムソン散乱
- まとめ

Doppler Reflectometer

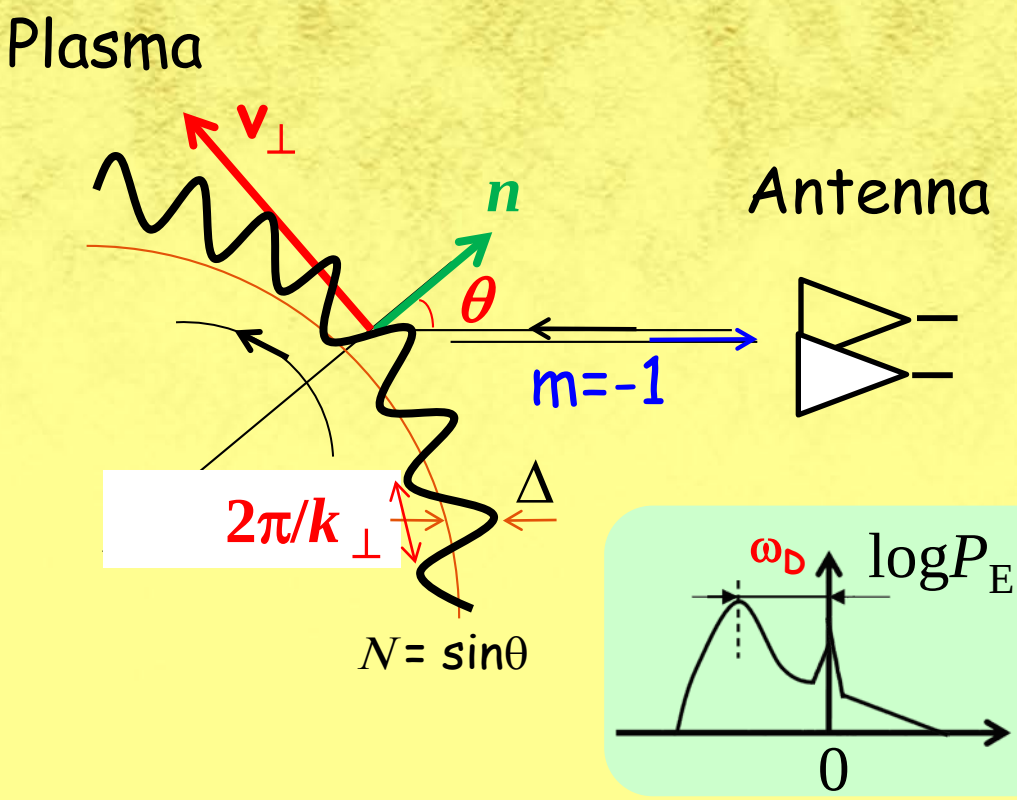

- wave vector is selected via Bragg condition :

$$k_\perp = 2 \cdot k_0 \sin(\theta)$$

- k-spectral resolution is defined by beam width :

$$\Delta k_\perp = \frac{2\sqrt{2}}{w}\sqrt{1+\left(\frac{w^2 k_0}{\rho_{eff}}\right)^2}$$

- Doppler Shift:

$$\omega_D = -\mathbf{k}\cdot\boldsymbol{\upsilon}$$

$$\approx -k_\perp \upsilon_\perp$$

$$\upsilon_\perp = \upsilon_{phase} + \upsilon_{E\times B}$$

strong points

- **Observation wave number is selectable in ITG/TEM turbulence region.**
- **No request for special heating operation**

Example of Doppler RM measurement (Comparison of regular & reverse magnetic field direction)

- When the direction of magnetic field is inversed, the sign of Doppler shift frequency is also changed.

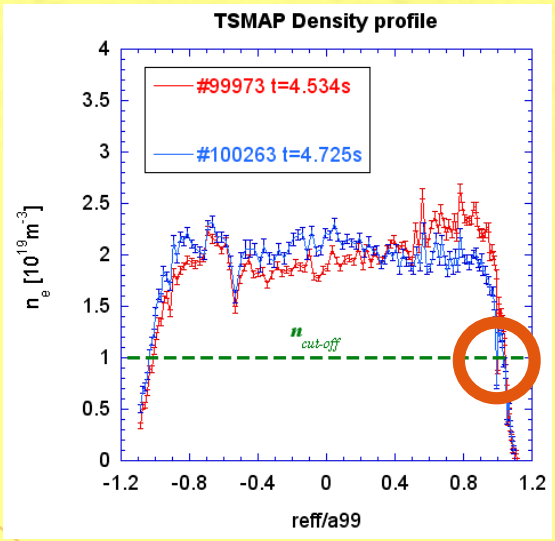

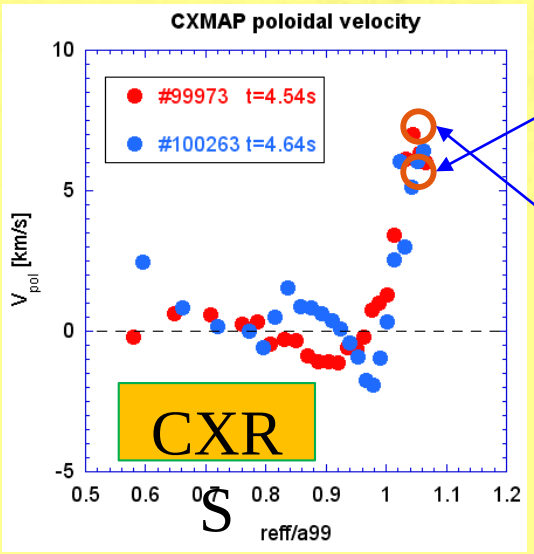

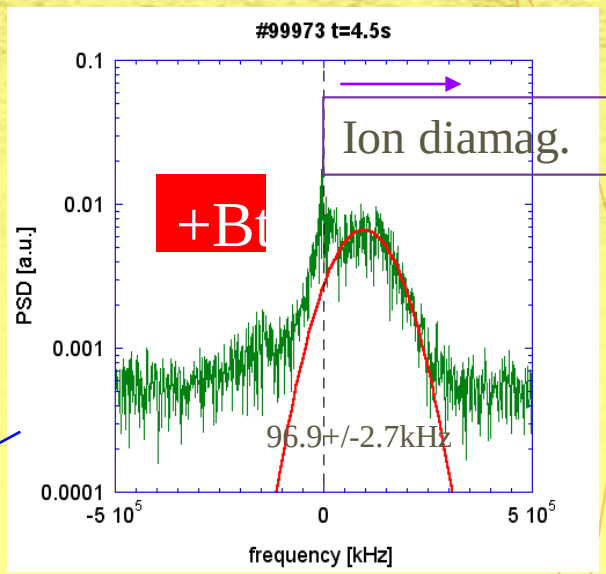

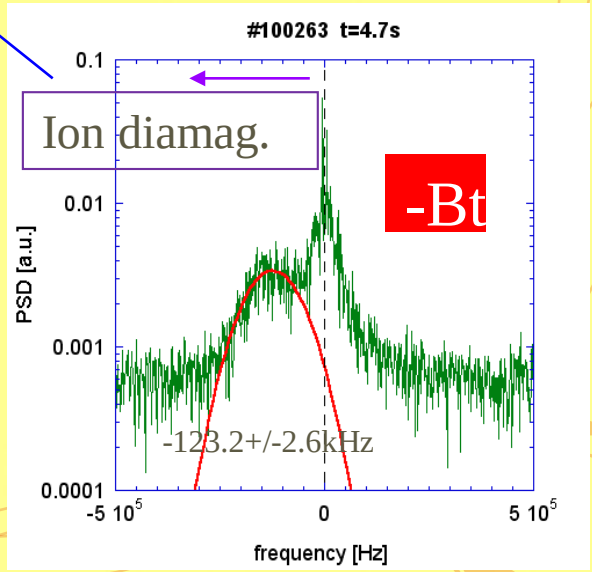

- #99973 5.8±0.1km/s
- #100263 7.2±0.1km/s

How to make "multi-frequency channel" ?

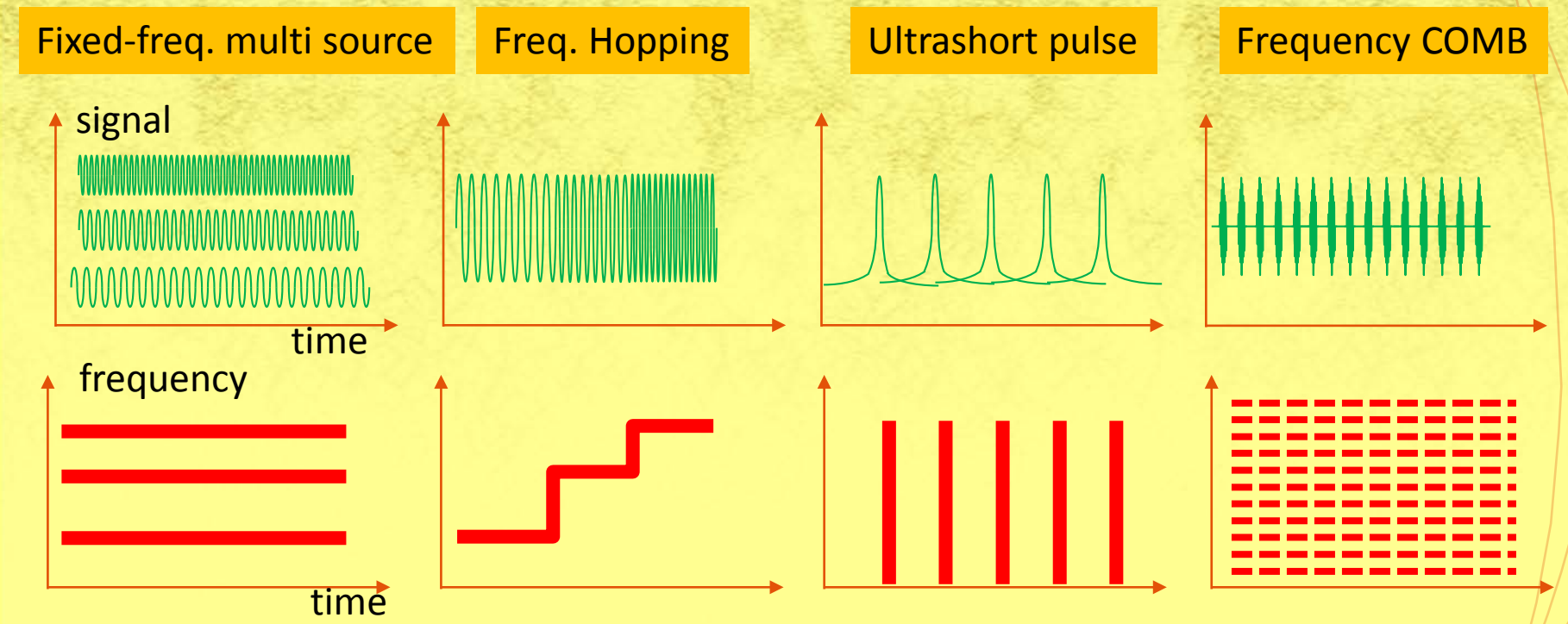

✓ "**Simultaneous**" measurement for studying the spatio-temporal behavior

ka-band 7ch frequency comb reflectometer in LHD

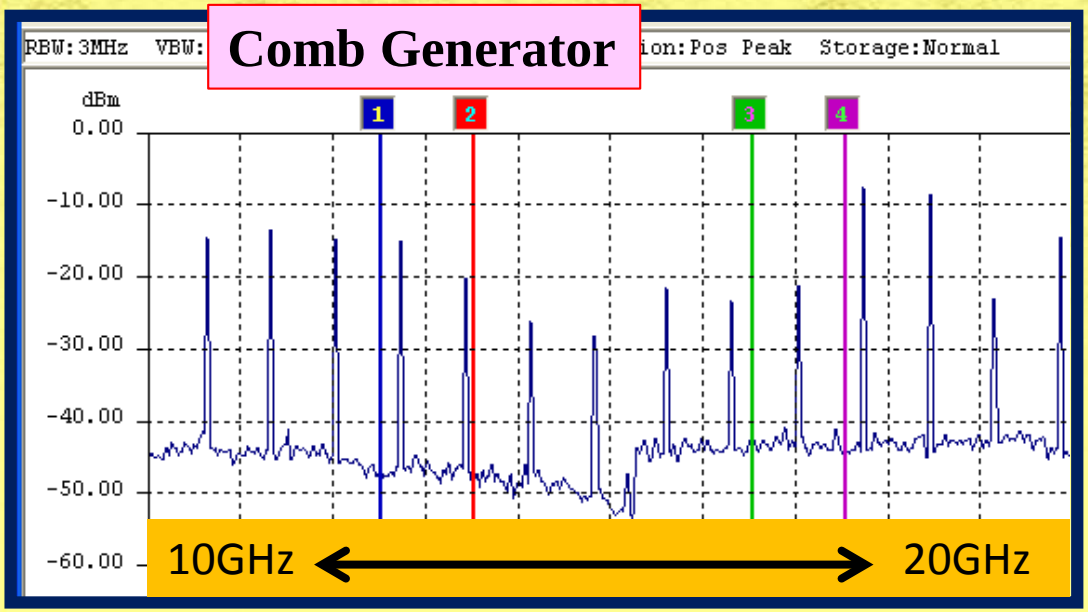

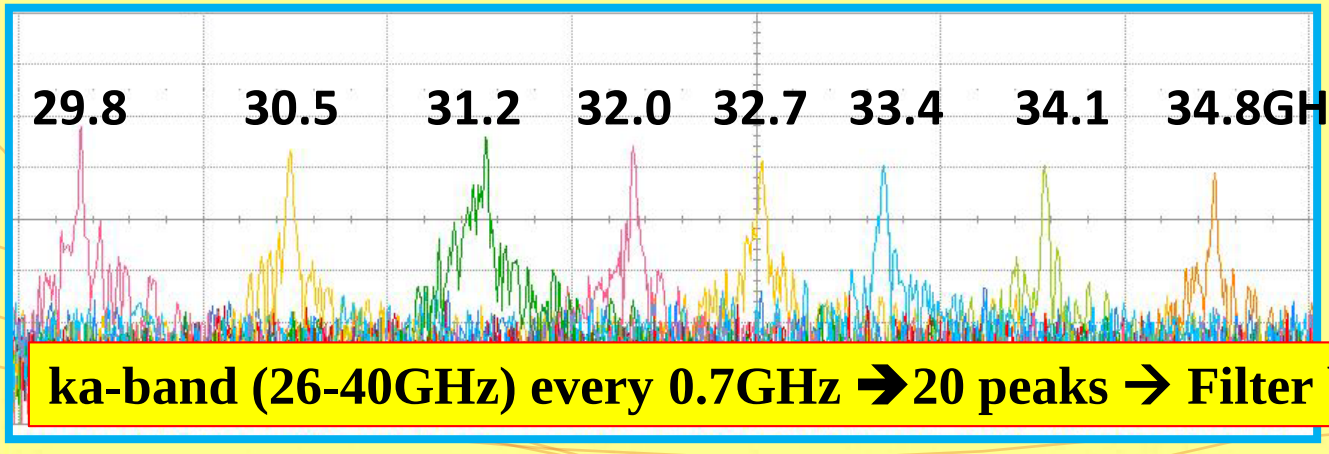

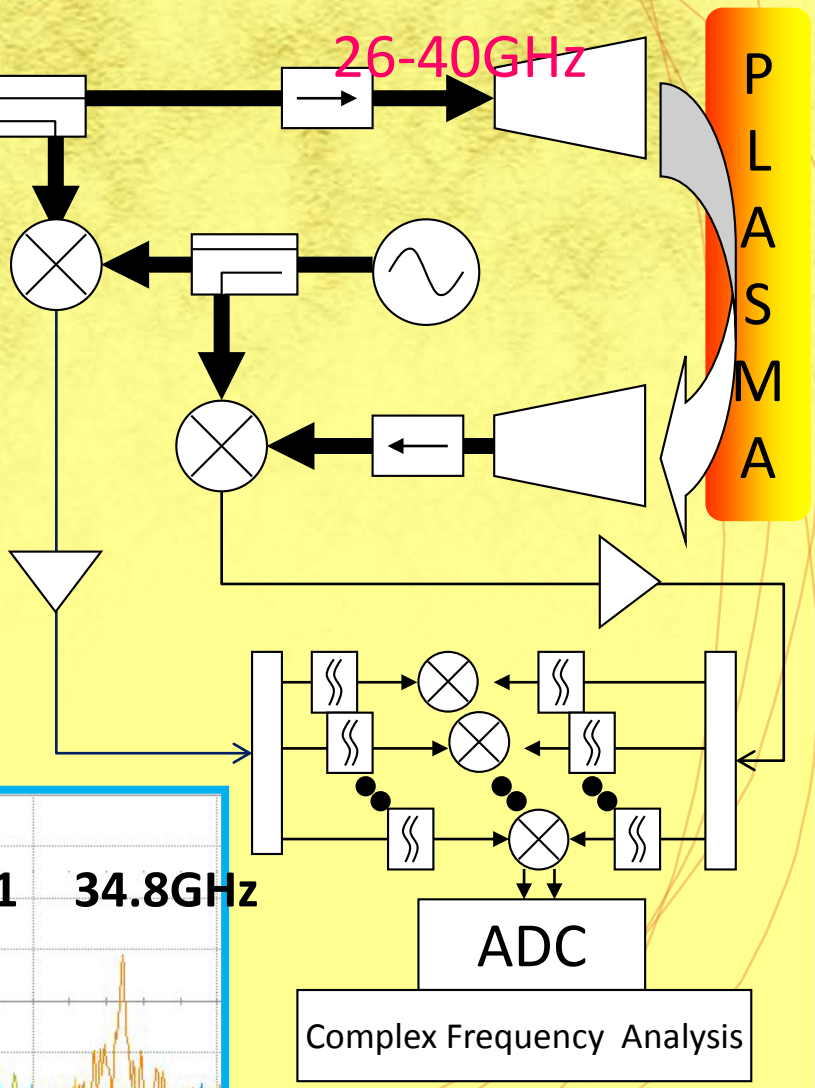

ka-band (26-40GHz) every 0.7GHz → 20 peaks → Filter bank system (7ch)

up to 20ch

Radial electric field Er is controlled by the biasing electrode

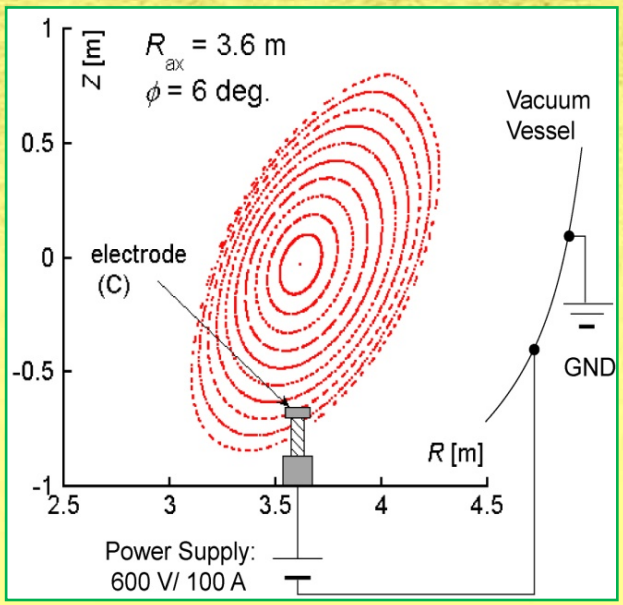

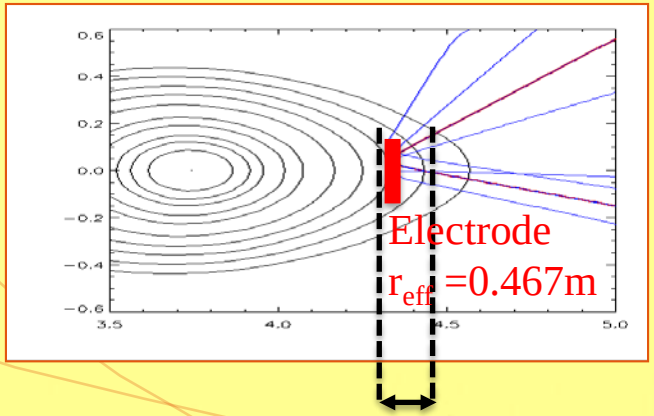

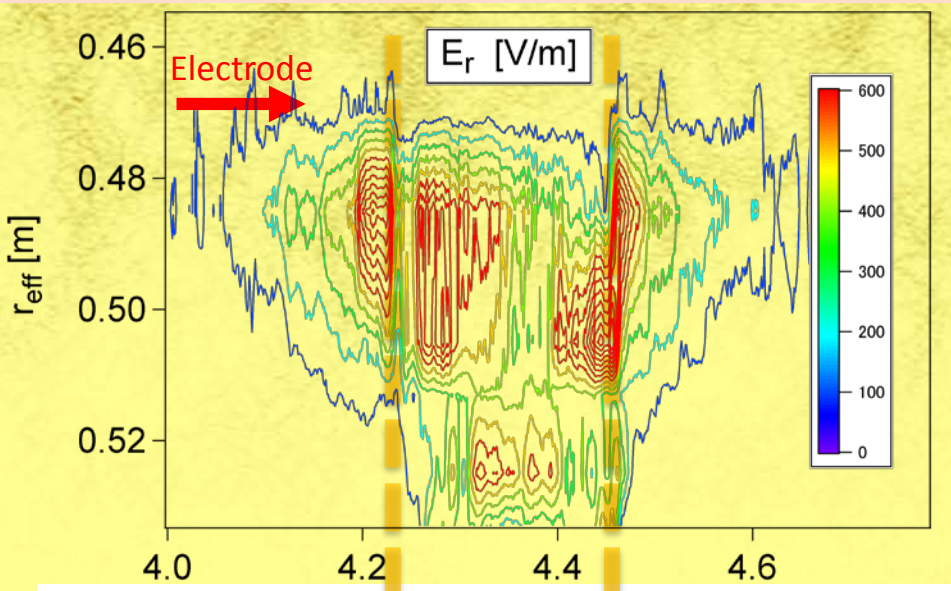

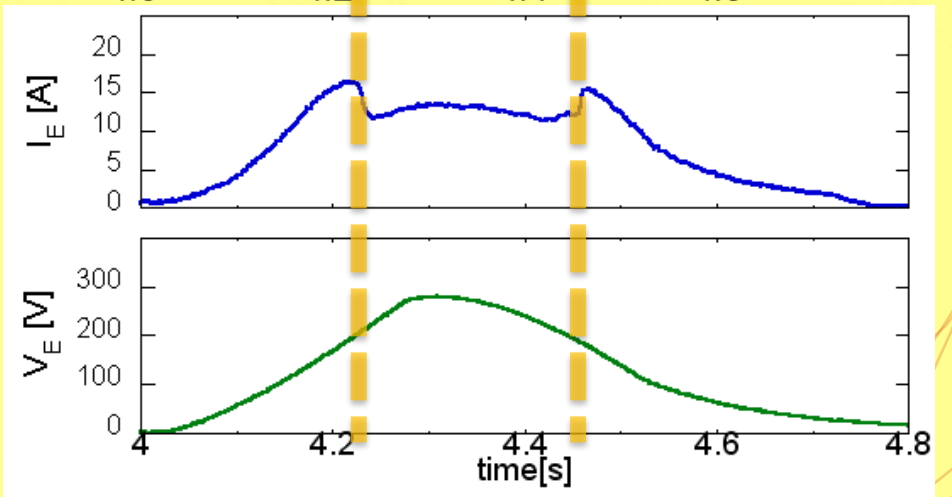

ECH:0.8MW Reflectometer

r_{eff} ~ 0.45 ~ 0.53m

a_{99} ~ 0.58 m

Strong Er region jump outwards during ramp-up of bias voltage

Turbulence intensity correlates with -*Er Er''*

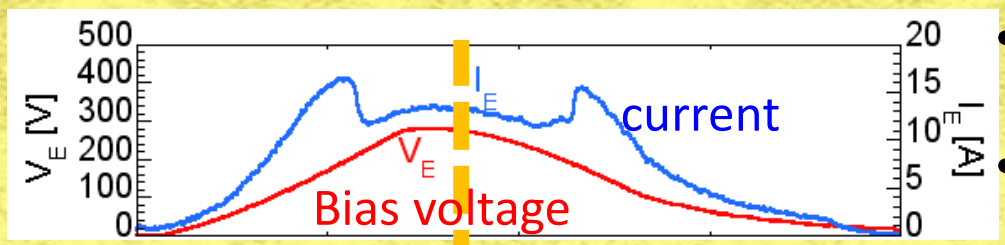

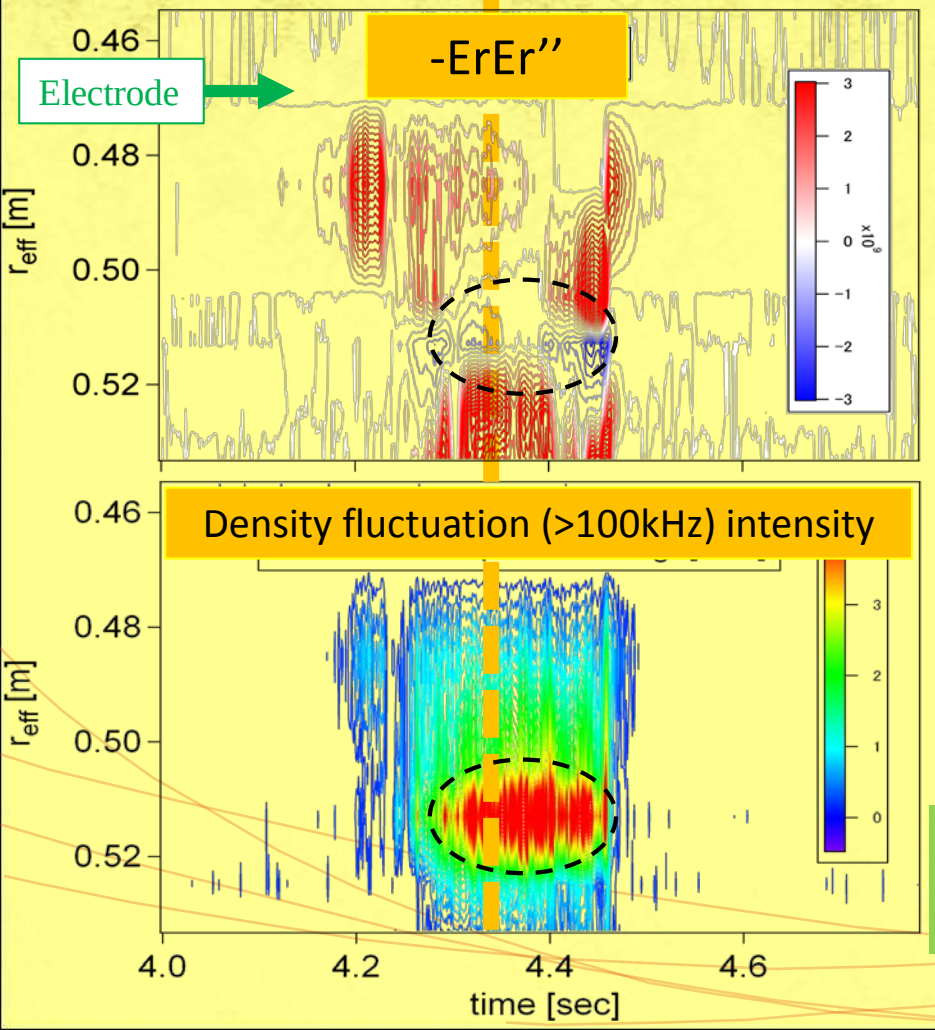

- The turbulence intensity enhanced in the region where $-Er\,Er'' < 0$.
- The turbulence intensity does not correlate with *Er'*.
- The results are not conflicted with the theory on the importance of -*Er Er''*.

$$\frac{\partial}{\partial t} I = \gamma I - \omega_2 I^2 - \alpha\left(-E_r E_r''\right) I$$

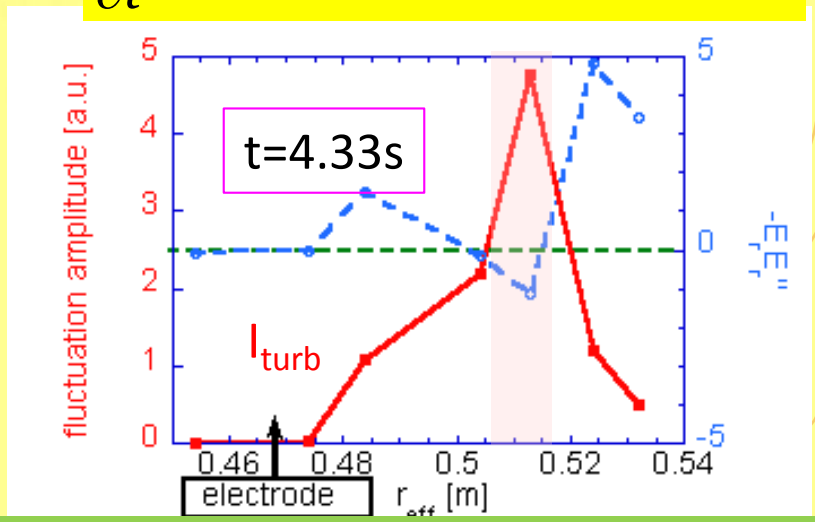

Meso-scale Er [Er'']is important for turbulence reduction

T.Tokuzawa PoP 21, 055904 (2014)

Target parameters of Doppler RM

① Doppler shifted frequency

→ poloidal velocity

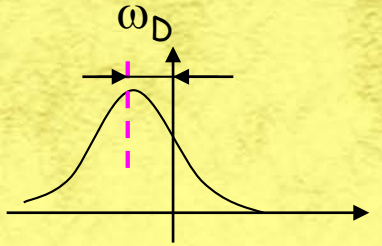

$$\omega_D = -\mathbf{k}\cdot\boldsymbol{\upsilon}$$
$$\approx -k_\perp \upsilon_\perp$$

② Integration in frequency domain

→ wave number spectrum

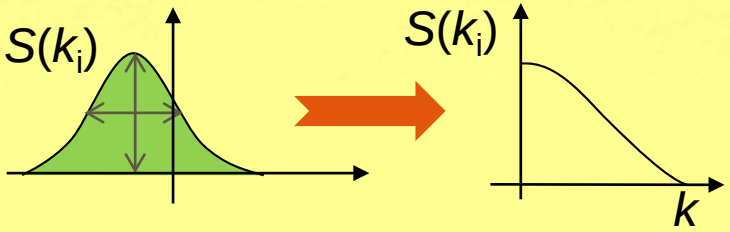

③ Temporal behavior of Doppler shift frequency

→ velocity / frequency of background plasma（zonal flow, GAM, etc.）

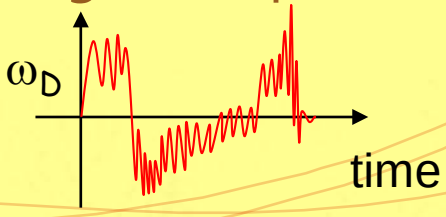

ゾーナル流(GAM)計測

Geodesic Acoustic Modes

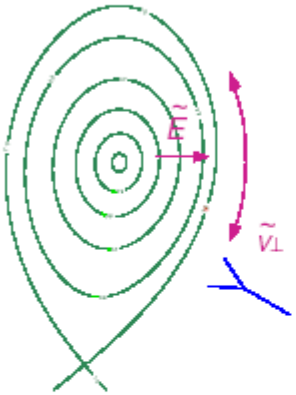

周波数スペクトル

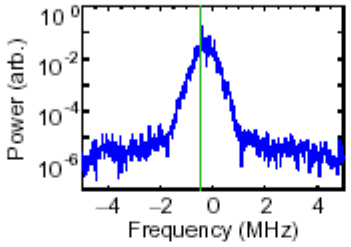

ドップラーシフトした周波数の時間変化

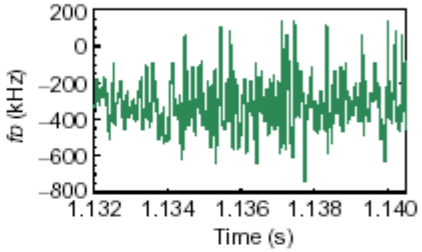

56GHz x-mode Doppler refl.

- Ohmic shot #16179
  ρ ~ 0.98, *Te* ~ 120eV

FFT

- Electrostatic (low *m*) acoustic mode, i.e. $\tilde{B} = 0$
- Low frequency. Large $\tilde{E}$, even for small $\tilde{n}$
- Mechanism
  $\tilde{E} \rightarrow \tilde{v}_\perp = \tilde{E} \times B/B^2$ and $\tilde{n} \propto -\nabla \cdot \tilde{v}_\perp$
  $\tilde{n} \rightarrow \tilde{J} = B \times \nabla \tilde{n}$ which transports charge
  → acts against $\tilde{E}$ → "poloidal" oscillation
- Linked with zonal flows, predicted by codes

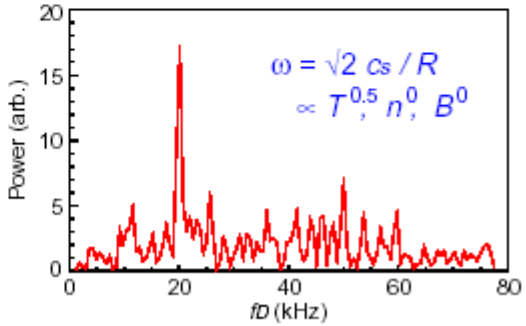

G.D.Conway, 05-May-03 IRW6-t12

- 背景流(~径電場)の揺らぎを計測。

Ultrashort Pulse

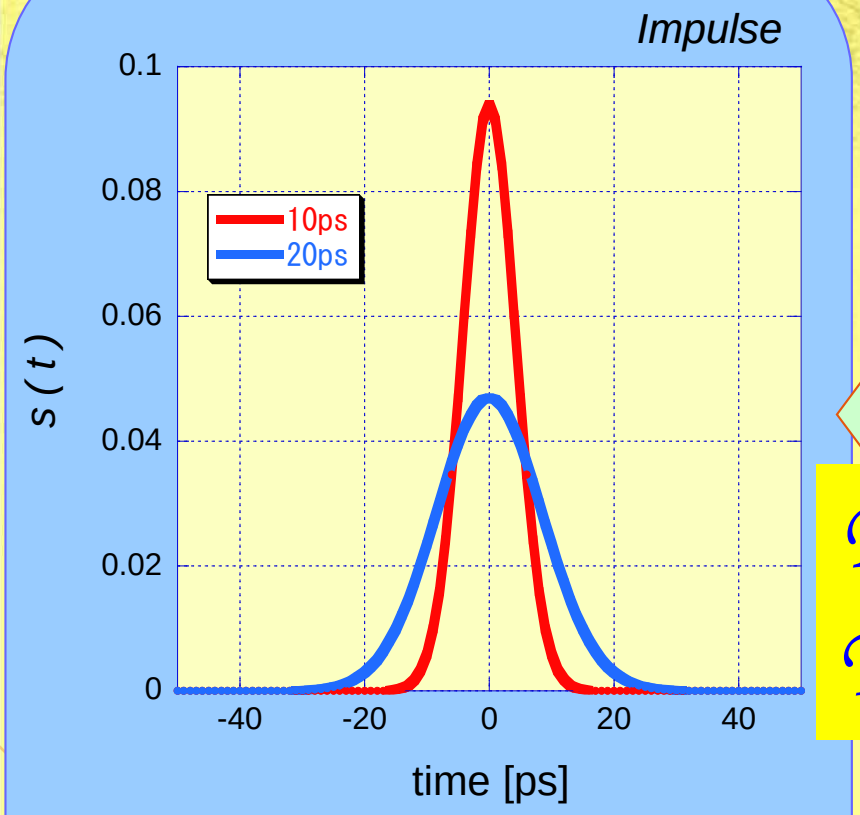

$$s(t) = \frac{1}{\sqrt{2\pi}\sigma}\exp\left(-\frac{t^2}{2\sigma^2}\right)$$

Fourier Transform

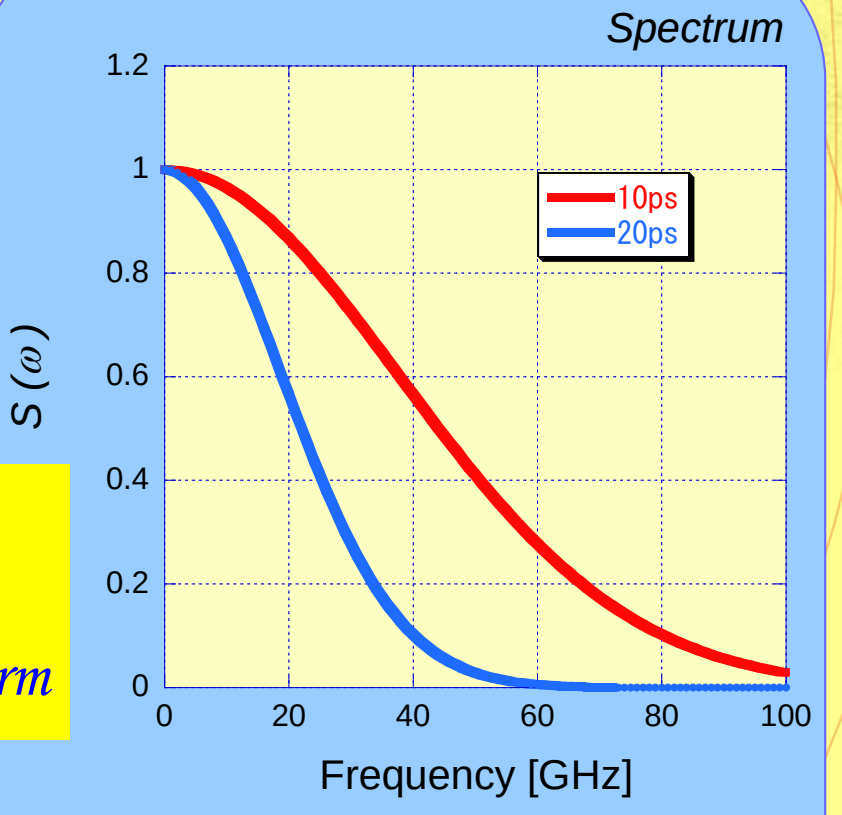

$$S(\omega) = \exp\left(-\frac{\omega^2\sigma^2}{2}\right)$$

Example of Reflected Signal

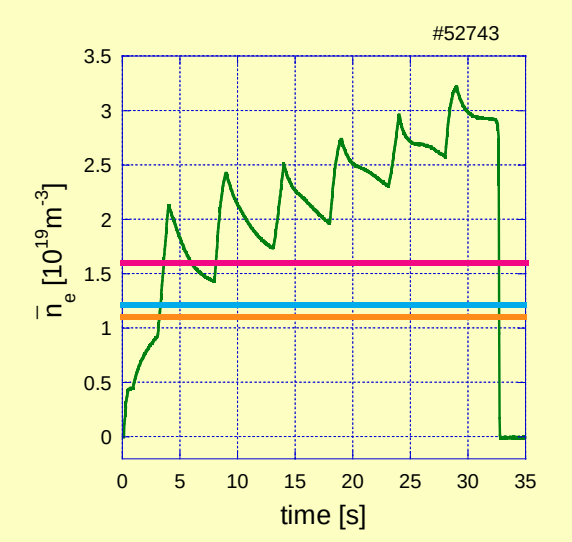

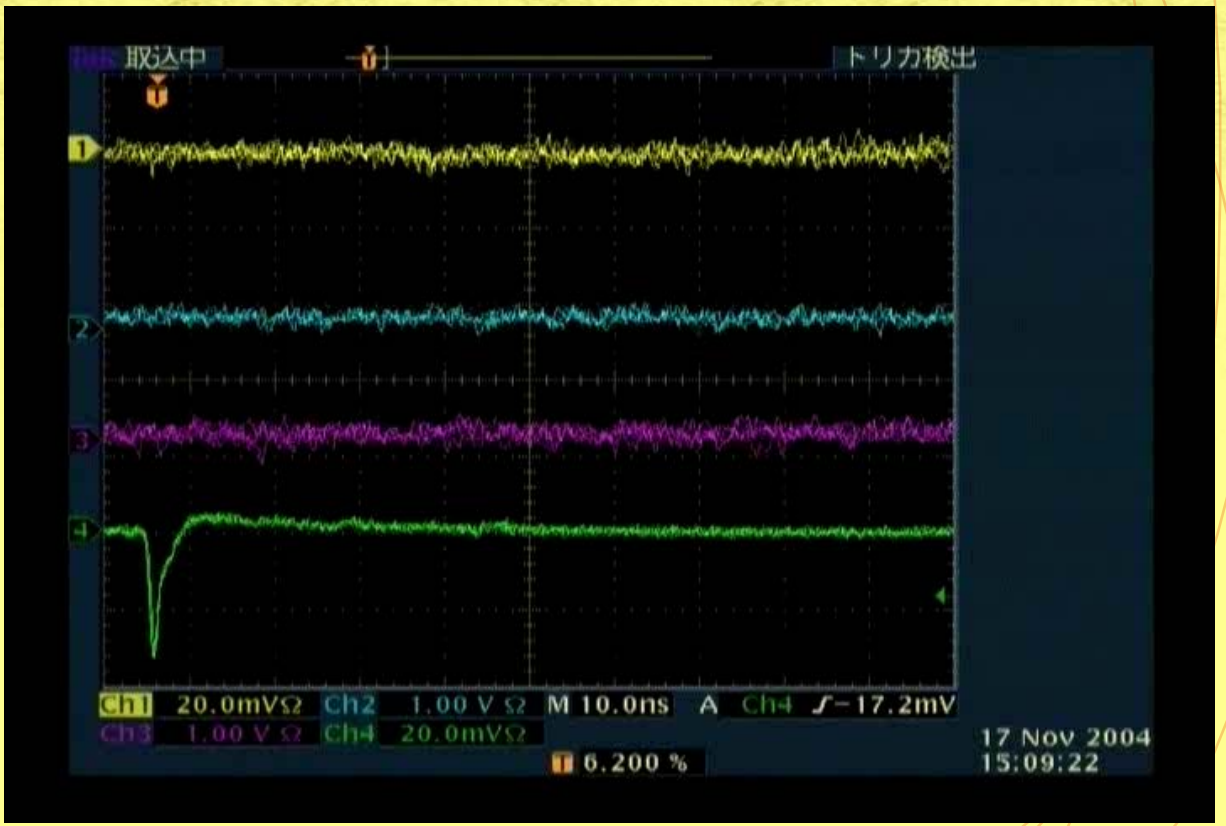

Yellow : 31GHz
Blue : 32GHz
Red : 36GHz
Green : Reference

Density Profile Measurement

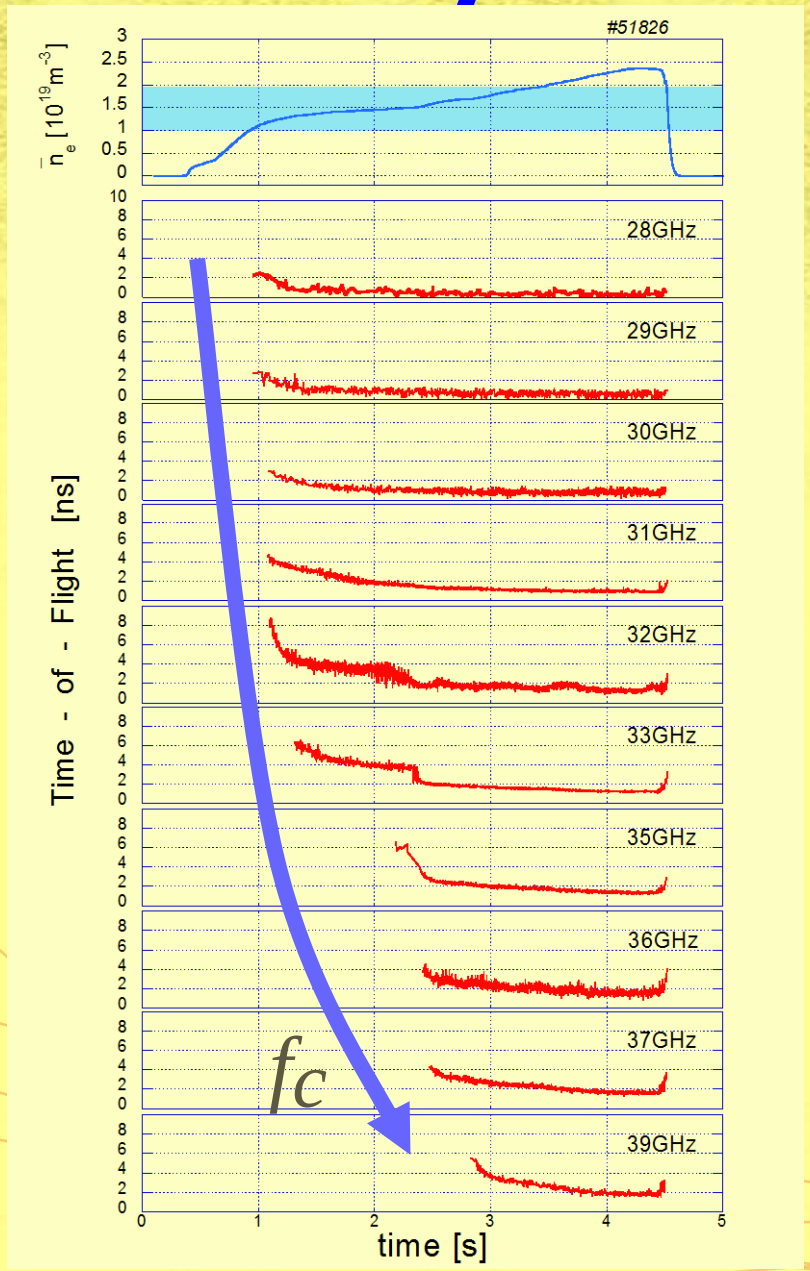

Reconstructed ne profile

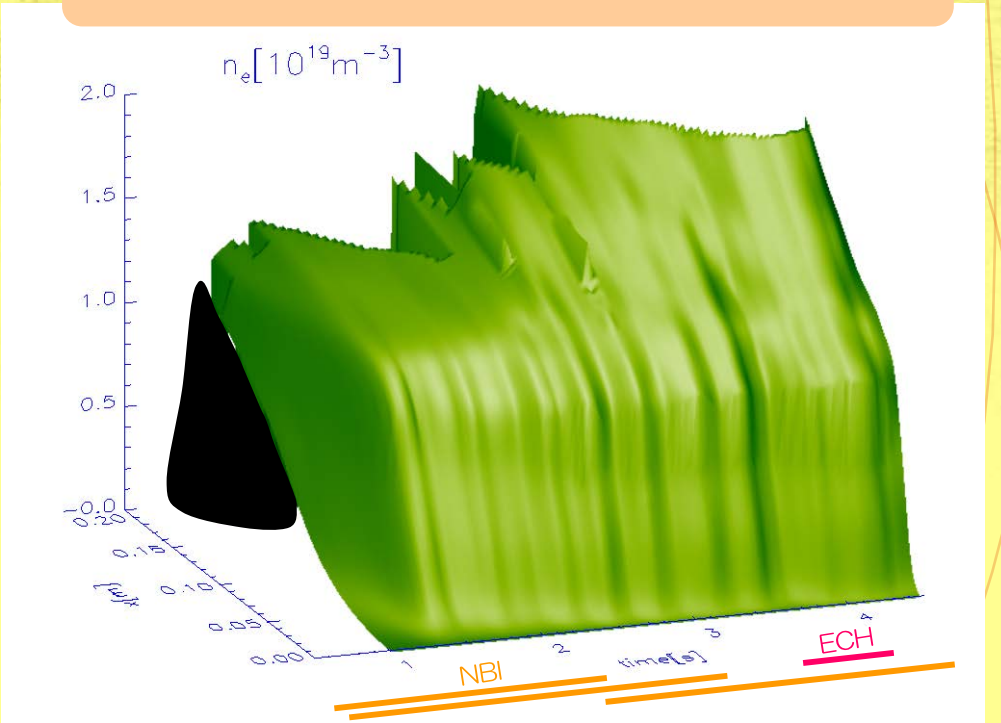

- Here, time-of-flight is defined by the traveling time between plasma edge and each cutoff layer.
- Each reflected pulse is appeared, when the corresponding cutoff layer is generated in the plasma.

Edge position monitor in LHD

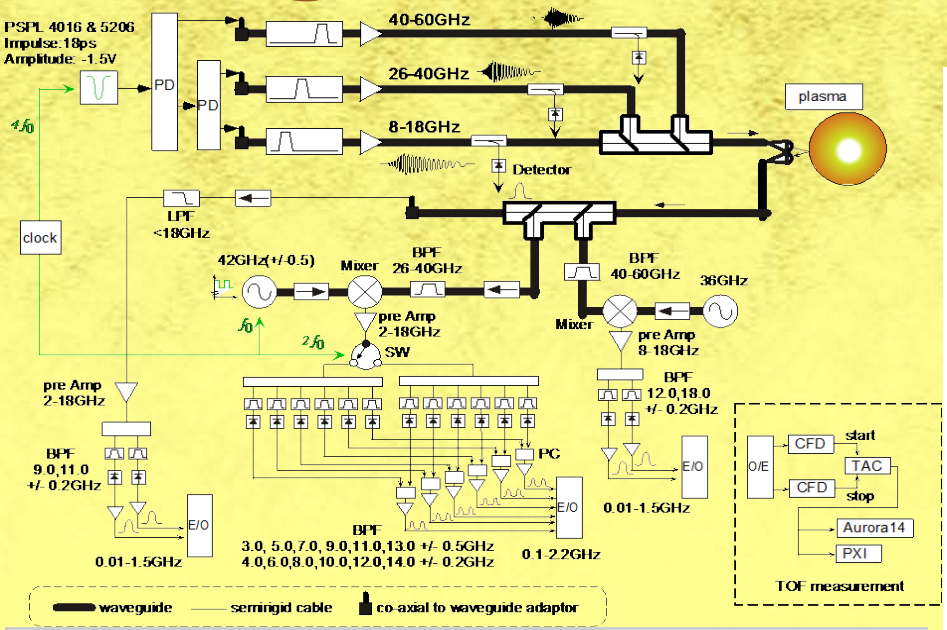

- Impulse (23ps pulse width) is used as a broad band source (8-60GHz).
- Time-of-Flight measurements are done for density profile measurement.

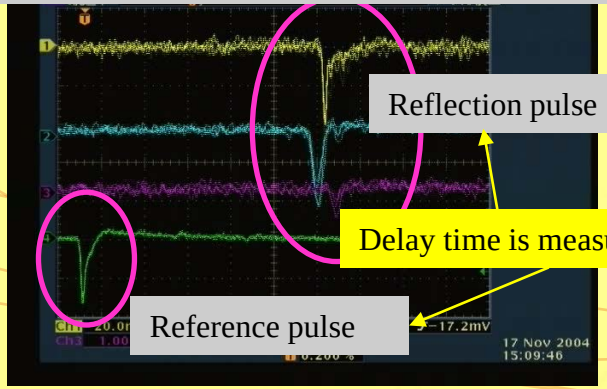

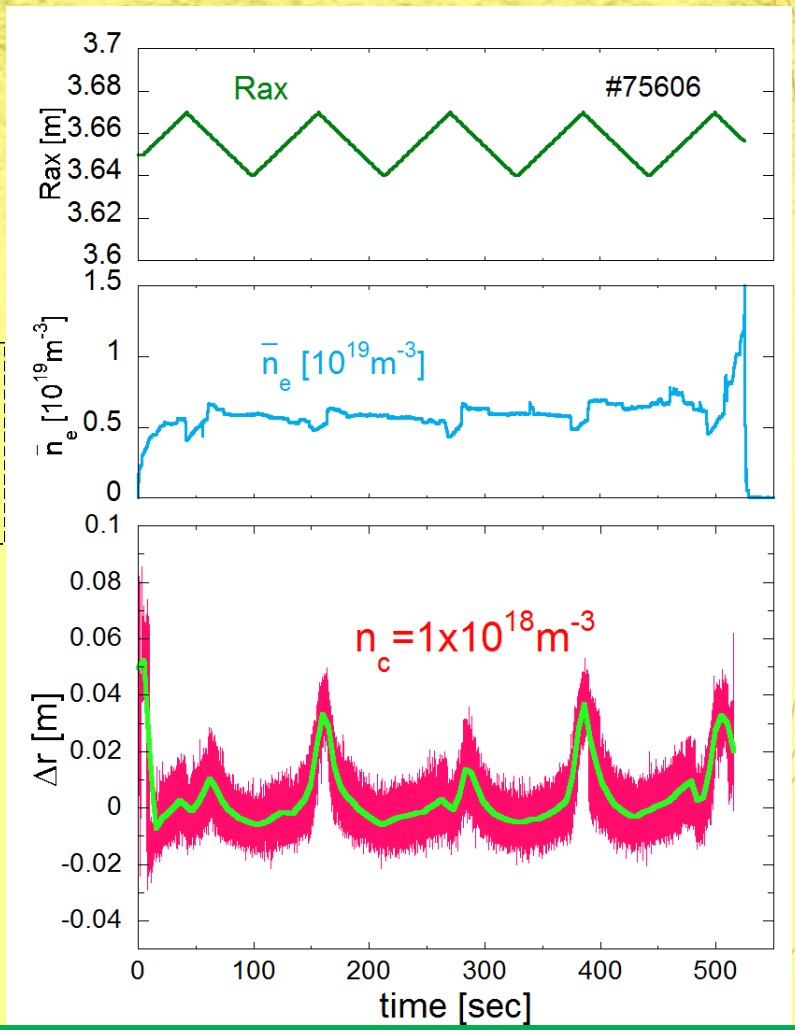

1x$10^{18}m^{-3}$の密度層の位置を
～500secにわたり、精度<1cmで計測可能

テラヘルツ波パルスを用いた計測をすると

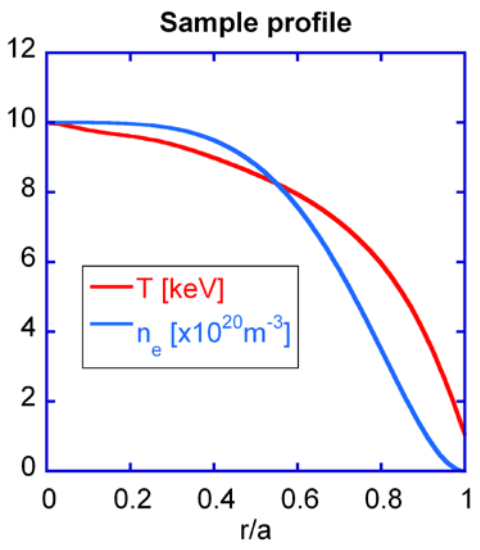

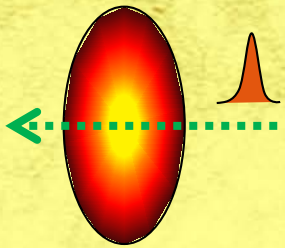

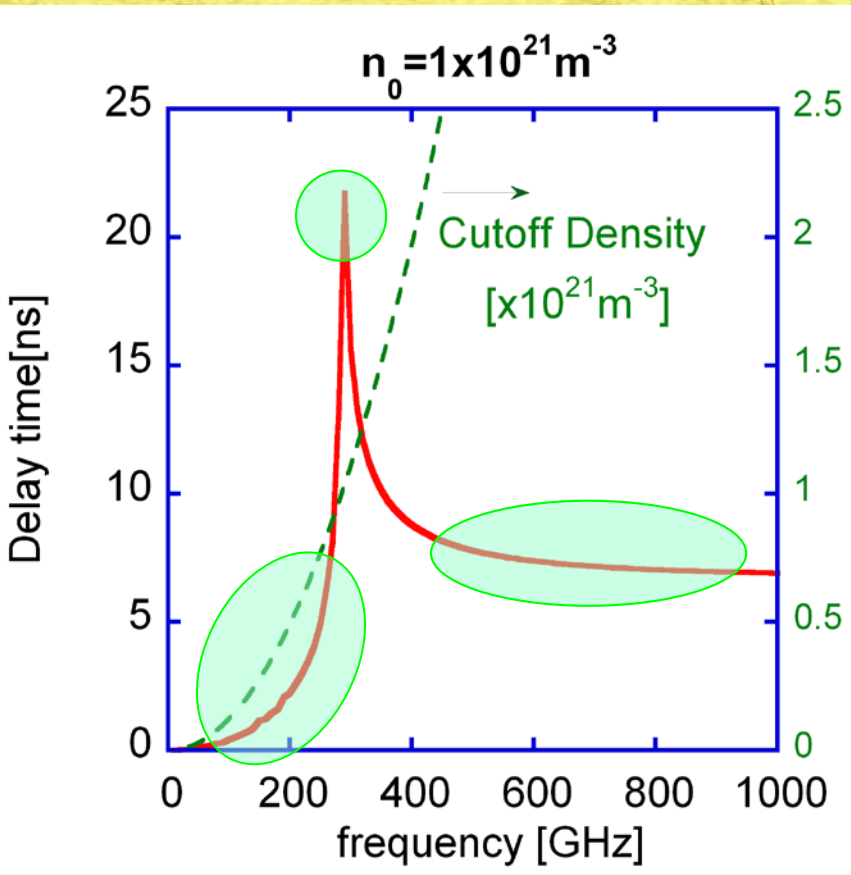

- カットオフ周波数よりも高いプローブ周波数を用いたDelayometry計測から
  ➡ **線平均密度** $\overline{n}_e$
- 広帯域周波数をプローブすることで、Delay timeが最大となる周波数から
  ➡ **ピーク密度** $n_{e\_\max}$
- 最大カットオフ周波数以下の信号による反射計測から
  ➡ **密度分布** $n_e(\rho)$

メリット:
- 原理的に位相トビがない。
- 計測値の履歴が不要。
  ➔ **長時間運転時に重要**

NIFS THz-TDS system

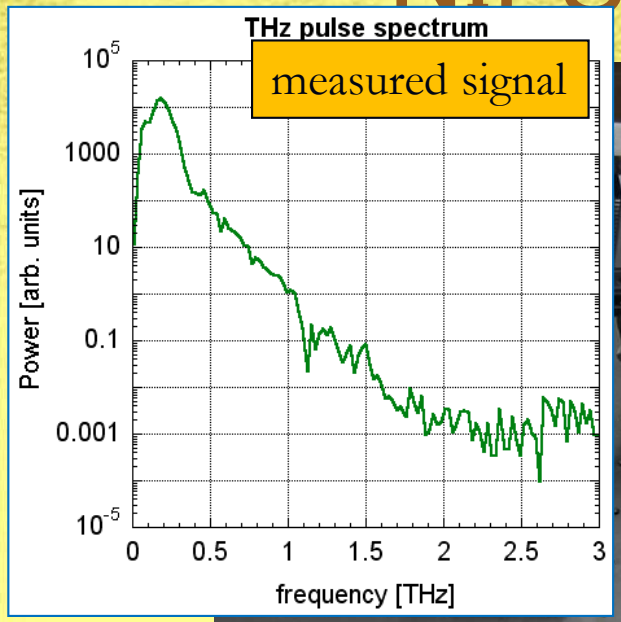

Hamamatsu Photonics K.K.
model: G10620-12 (bow-tie)

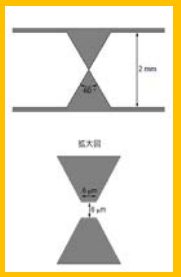

Spectrum

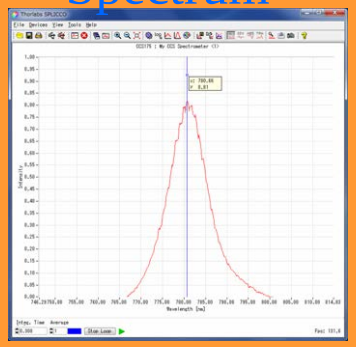

λ=780nm+/-4.8nm
P_{output}=79.3mW
PulseWidth=120fs

NT60/65
stroke : 65mm
resolution : 0.1um
speed : 1000mm/s

Contents

- はじめに
- 干渉計
  - マイクロ波干渉計、FIRレーザー干渉計、分散干渉計
- 反射計
  - ドップラー反射計、パルスレーダー
- 協同トムソン散乱
- まとめ

Collective Thomson scattering geometry

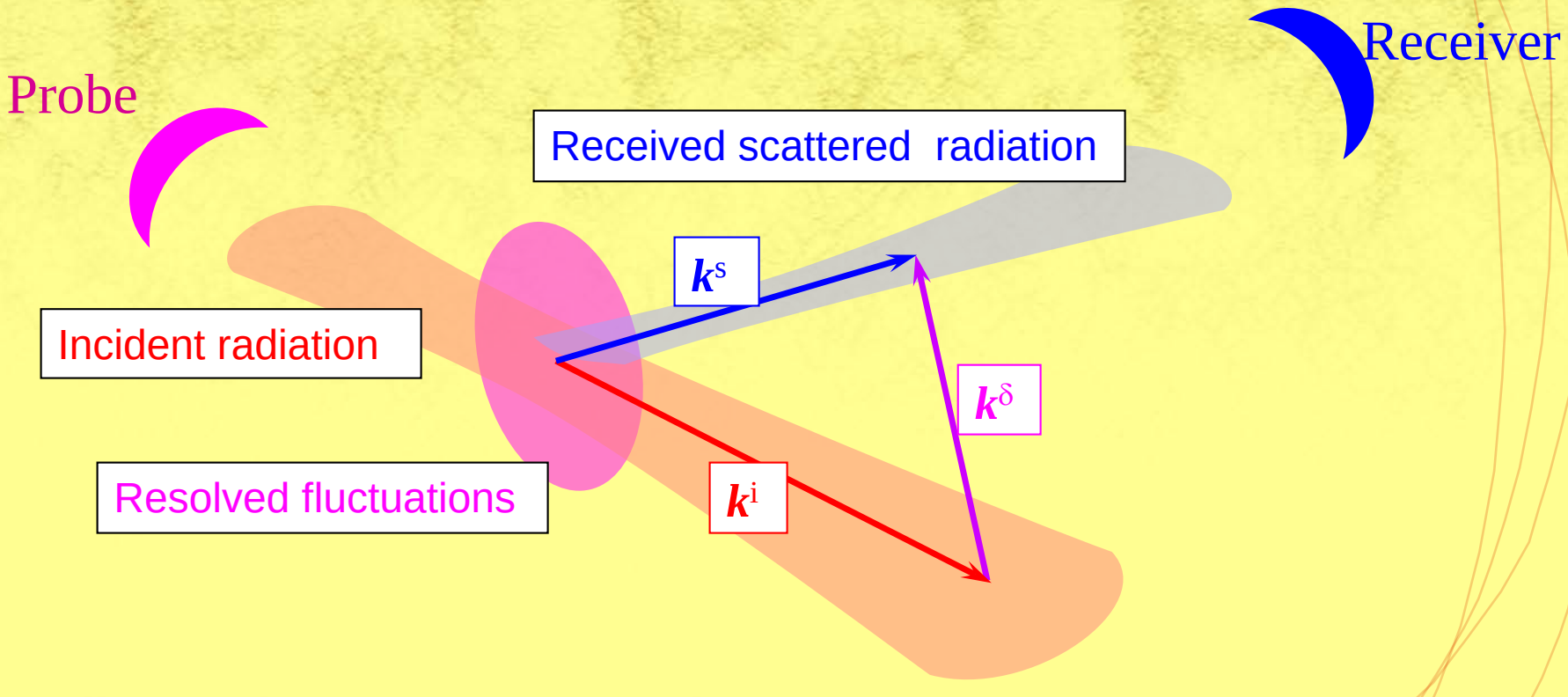

Collective Thomson scattering resolves velocity component along $\boldsymbol{k}^\delta$:

$$f^{(1)}(u) = \int \delta\left(u - \hat{\mathbf{k}}^\delta \cdot \mathbf{v}\right) f(\mathbf{v})\, d\mathbf{v}$$

Feature of CTS spectrum for electrons, ions, and fast ions

- Scattered radiation is written as

$$P_s \propto n_e S(k,\omega) = \text{Electron} + \text{Ion} + \text{Fast Ion}$$

$$S(k,\omega) = \left|1-\frac{H_e}{\varepsilon_L}\right|^2 \frac{2\pi^{1/2}}{|k_\parallel| v_e} \sum_{l=-\infty}^{\infty} \exp\left(-k_\perp^2\rho_e^2\right) \mathrm{I}_l\left(k_\perp^2\rho_e^2\right) \exp\left(-\frac{(\omega - l\Omega_e)^2}{k_\parallel^2 v_e^2}\right)$$

$$+ \left|\frac{H_e}{\varepsilon_L}\right|^2 \frac{2\pi^{1/2} Z_i^2 n_i}{n_e |k_\parallel| v_i} \sum_{l=-\infty}^{\infty} \exp\left(-k_\perp^2\rho_i^2\right) \mathrm{I}_l\left(k_\perp^2\rho_i^2\right) \exp\left(-\frac{(\omega - l\Omega_i)^2}{k_\parallel^2 v_i^2}\right)$$

$$+ \left|\frac{H_e}{\varepsilon_L}\right|^2 \frac{2\pi Z_{ene}^2 n_{ene}}{n_e |\vec{k}| v_{ene}} f_{ene}^{(1)}\left(\frac{\omega}{k}\right)$$

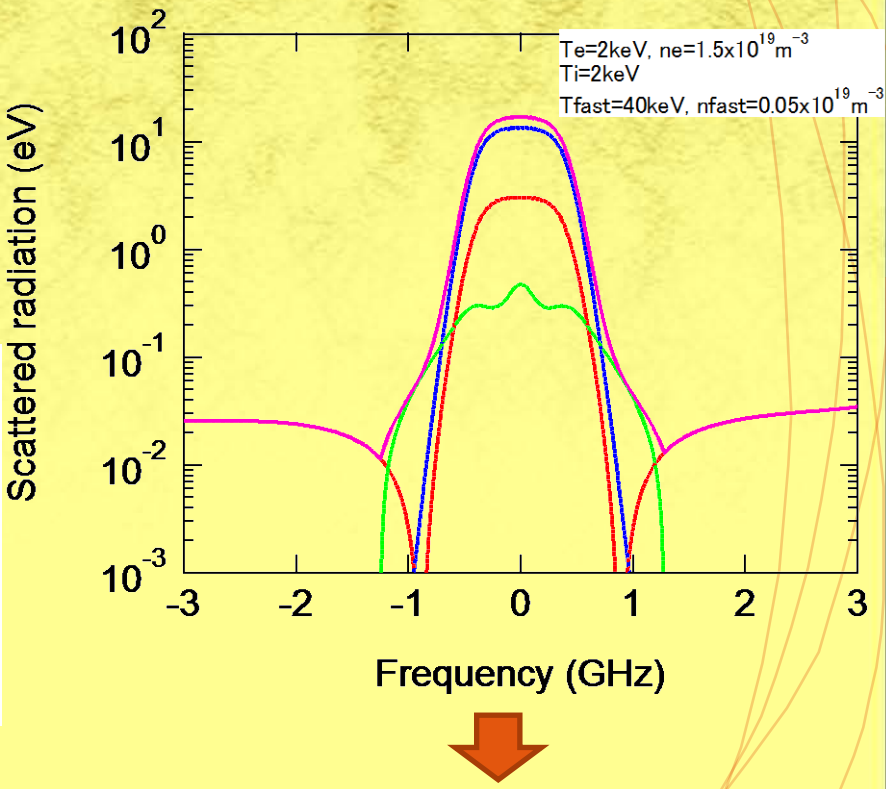

In collective regime, the CTS spectrum spread is dominated by the ion feature.

Measured frequency shift corresponds to the charged particle velocity.

The distribution function is obtained from measured CTS spectrum.

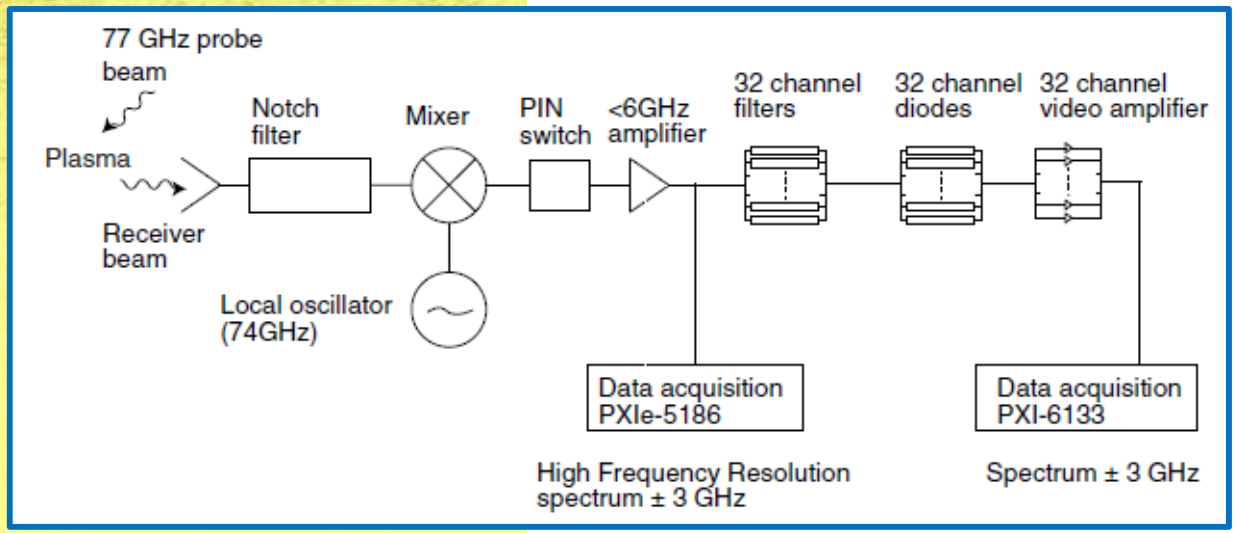
77 GHz probe beam
Plasma
Receiver beam
Notch filter
Mixer
PIN switch
<6GHz amplifier
32 channel filters
32 channel diodes
32 channel video amplifier
Local oscillator (74GHz)
Data acquisition PXIe-5186
Data acquisition PXI-6133
High Frequency Resolution spectrum ± 3 GHz
Spectrum ± 3 GHz

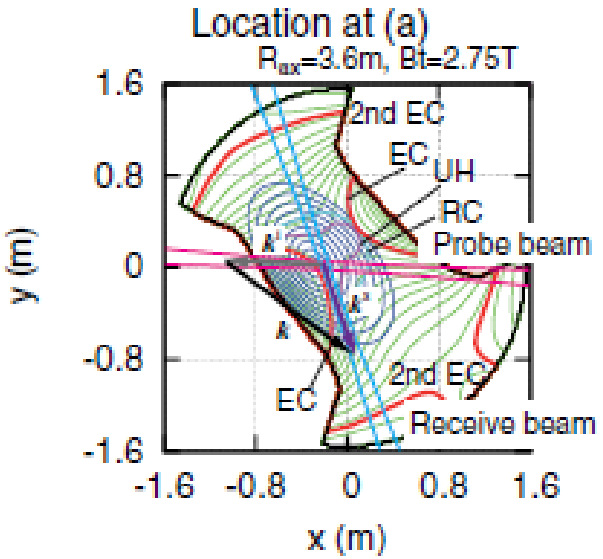
Location at (a)
R_{ax}=3.6m, Bt=2.75T
2nd EC
EC
UH
RC
Probe beam
2nd EC
EC
Receive beam
y (m)
x (m)

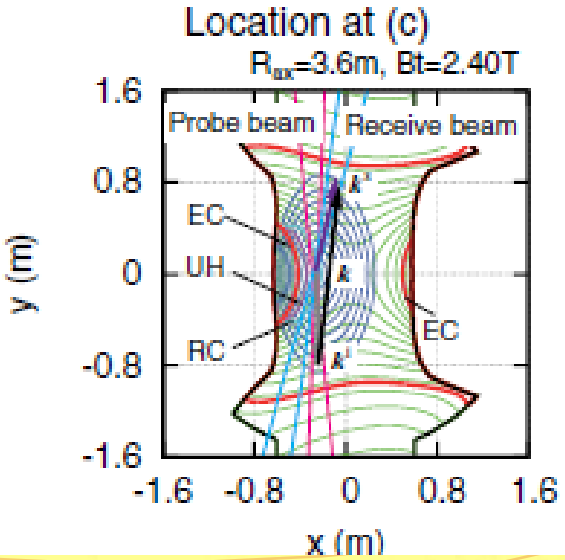
Location at (c)
R_{ax}=3.6m, Bt=2.40T
Probe beam
Receive beam
EC
UH
RC
EC
y (m)
x (m)

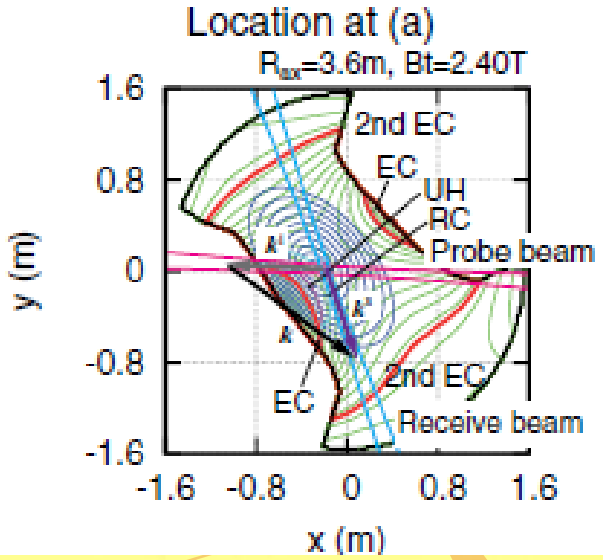
Location at (a)
R_{ax}=3.6m, Bt=2.40T
2nd EC
EC
UH
RC
Probe beam
2nd EC
EC
Receive beam
y (m)
x (m)

Measured CTS spectrum during NB injection

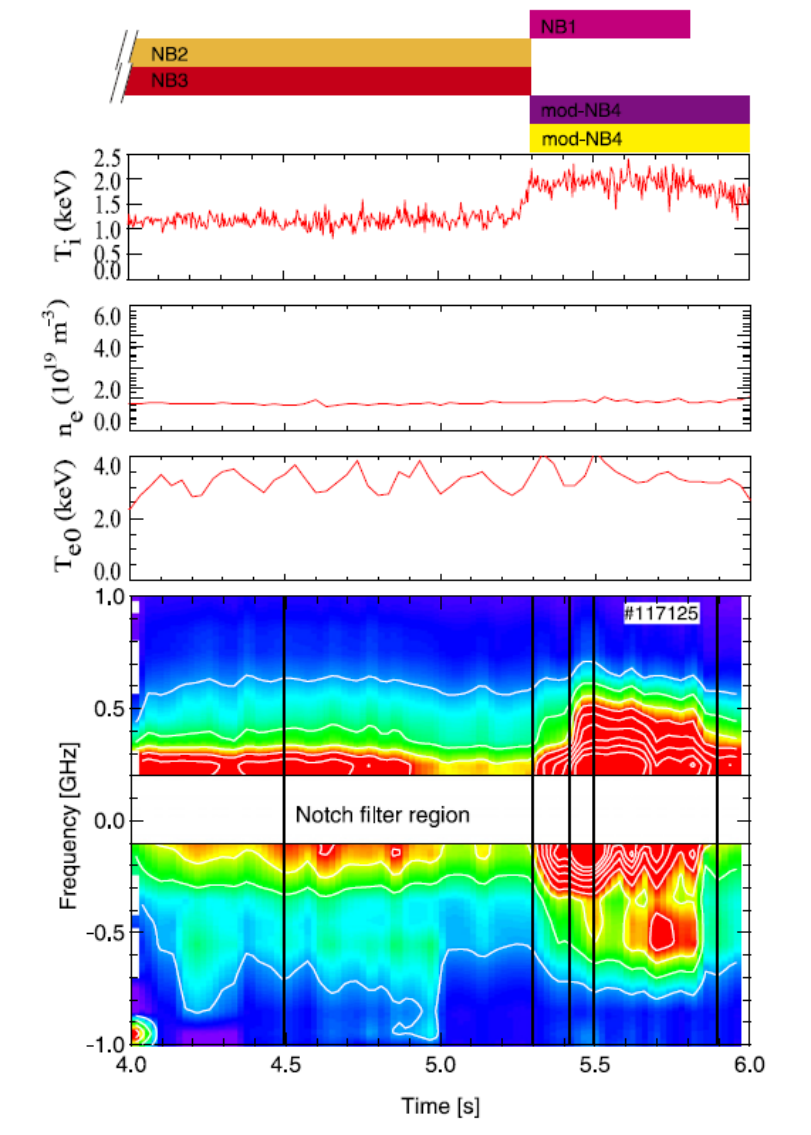

M. Nishiura *et al*

Nucl. Fusion **54** (2014) 023006

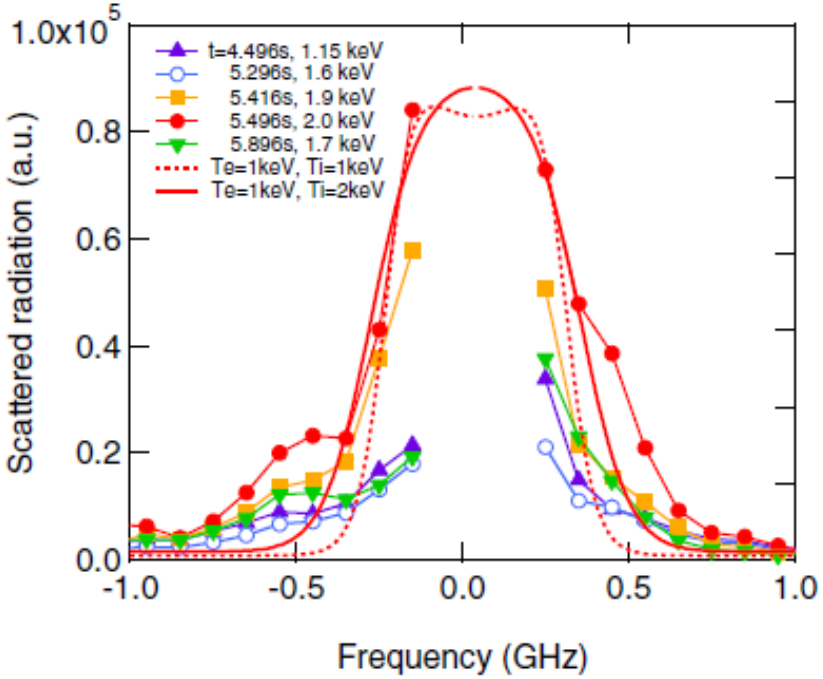

Figure 10. Measured CTS spectrum in the bulk-ion region. The measured T_i from Ar Doppler broadening is indicated for each time trend. The calculated CTS spectra are denoted by the dotted and the solid curves for $T_e = 1$ keV and $T_i = 1$ and 2 keV, respectively.

IBW in TEXTOR (CTS)

S. B. Korsholm, PRL **106,** 165004 (2011)

calculation

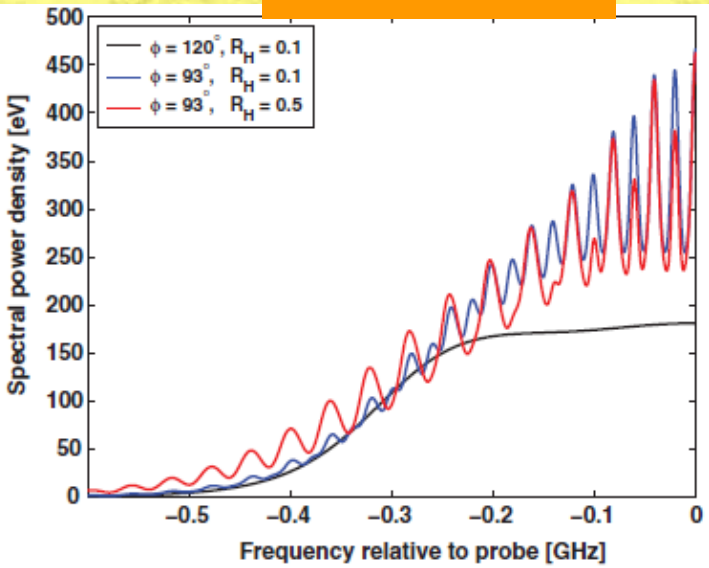

FIG. 1 (color). Calculated CTS spectra for a geometry with $\mathbf{k}^{\delta}$ close to perpendicular to $\mathbf{B}$, $\phi = 93°$ in a typical TEXTOR plasma for $R_H = 0.1$ (blue) and $R_H = 0.5$ (red). For comparison a calculated CTS spectrum for $\phi = 120°$ (black) and $R_H = 0.1$.

experiment

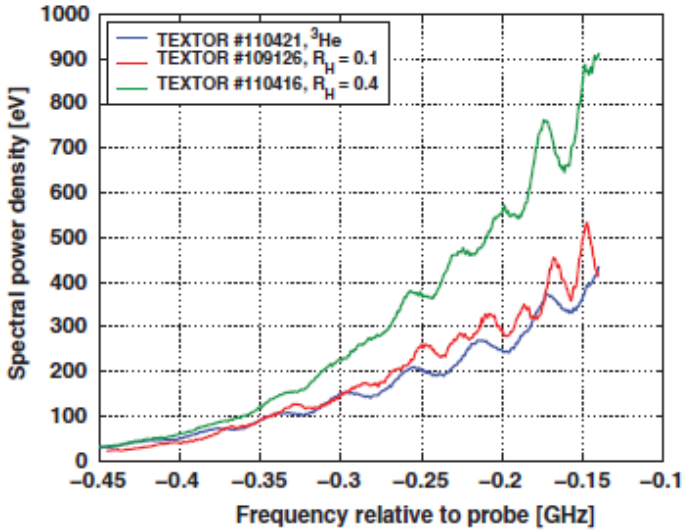

FIG. 3 (color). Measured CTS spectra in TEXTOR for a ^{3}He fueled plasma (green, discharge no. 110421), a deuterium dominated plasma (red, discharge no. 109126) and a plasma with 40% hydrogen (blue, discharge no. 110416). The spacing between the ICS peaks corresponds to the ion cyclotron frequencies of ^{3}He, D, and H, respectively.

- 元素によるIBW周波数の違いから、燃料比を推定する。

まとめ

精緻

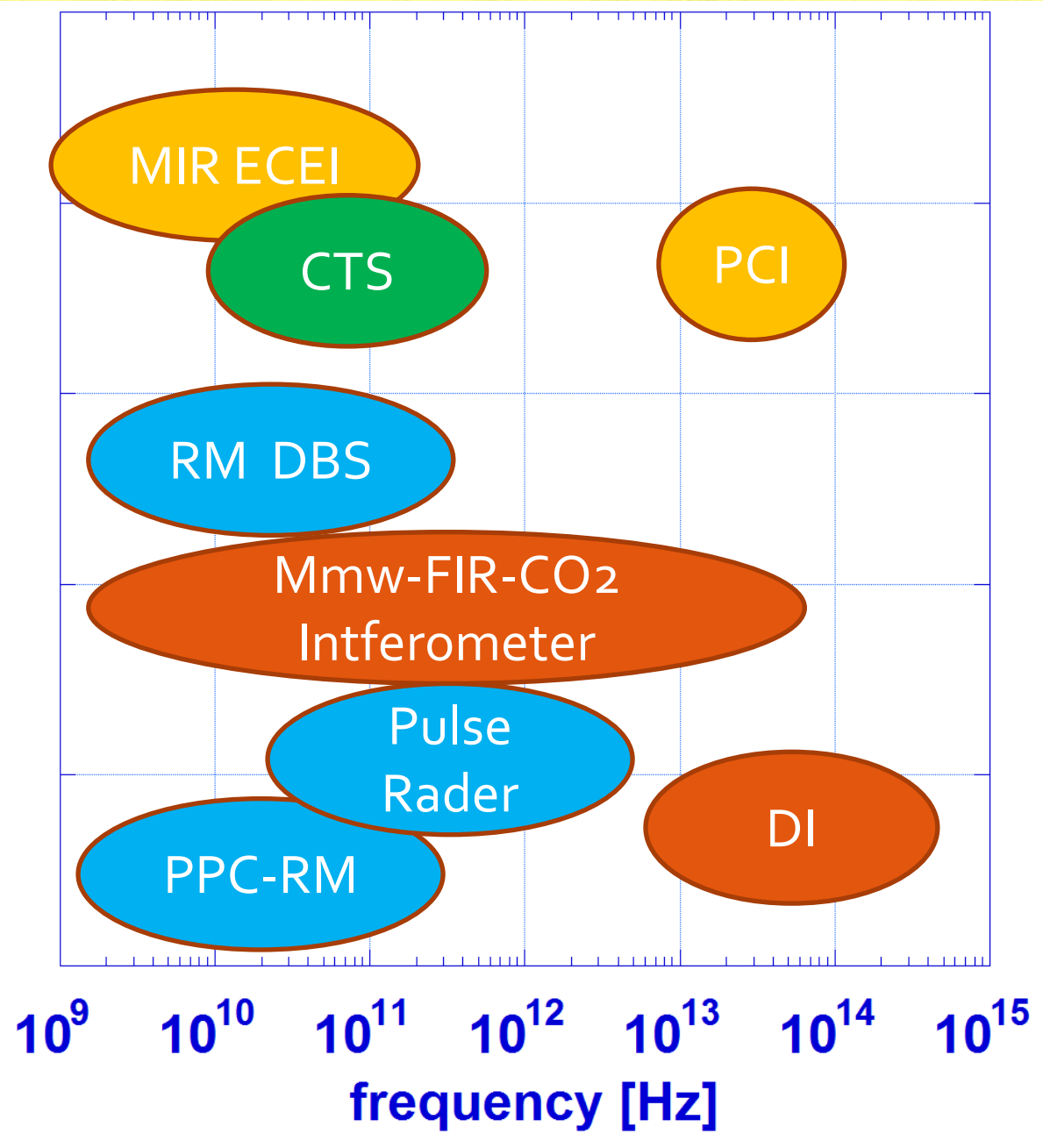
MIR ECEI
CTS
PCI
RM DBS
Mmw-FIR-CO2
Intferometer
Pulse
Rader
DI
PPC-RM
10^9
10^10
10^11
10^12
10^13
10^14
10^15
frequency [Hz]

安定

まとめ

- マイクロ波、ミリ波、テラヘルツ波という領域の電磁波を用いたプラズマ計測は、歴史が長い計測であり、技術は各種プラズマに最適化を施され、高度化・洗練されてきた。
- 今後の開発は2つの方向性になると思われる。一方は、先進的高精度化の方向性。もう一方は、プラズマ運転の、より直接的な制御ノブとしての計装化の方向性。

関連研究集会

- 「原型炉の運転制御に関するシンポジウム」
  - @3/12-13 : NIFS
- IRW12 （ International Reflectometry Workshop)
  - @5/18-20 (締切 : 3/27) ： Julich（ドイツ）
- ITPA-DG (計測)
  - @5/19-22 : NIFS
- LAPD2015 (Laser Aided Plasma Diagnostics)
  - @9/27-10/1 (締切 : 6/26) : 札幌